UNIVERISTY OF POLITEHNICA BUCHAREST

ȘCOALA DOCTORALĂ ȘTIINȚA ȘI INGINERIA MATERIALELOR

DOCTORAL THESYS

ENGLISH RESUME

STUDIES AND RESEACHES ON HIGH TEMPERATURE RESISTANT HIGH ENTROPY ALLOYS

PhD student: **Drd. Ing. Olaru Mihai Tudor**

Scientific coordinator: **Prof. Univ. Dr. Ing. Mihail Târcolea**

BUCUREȘTI 2020

Summary

Keywords: HEA, high entropy alloys, entropy, high temperatures, turbine engines, thermal power plants

Introduction

Transport and electricity generation are two major areas of global interest in terms of increasing the efficiency of the underlying processes. Although the emphasis has recently been on developing new technologies with a lower impact on the environment, fuel combustion processes are still the basis of energy generators: either electricity or energy needed for transportation.

The objective of this doctoral thesis is to obtain new sets of high entropy alloys specially designed for applications in systems that require high temperatures resistant materials. The use of new materials with improved properties for the manufacture of turbine blades of jet engines and combustion chambers in solid fuel power plants, helps to increase the combustion temperature in these systems and thus to increase efficiency, but also to reduce fuel consumption.

The doctoral thesis is structured in six chapters as follows:

Chapter 1 provides a theoretical foundation in the field of high entropy alloys and includes the specific effects of high entropy alloys, how they are formed and properties of alloys studied in the literature and ways to obtain them. Also, in the chapter are presented targeted applications where these alloys can bring improvements.

Chapter 2 presents design and modelling works of high entropy alloy compositions that will be studied later in Chapter 3. The chapter includes modelling the influence of Nb, Mo and W elements in alloy systems for the manufacture of turbine blades for jet engines as well as the influence of the elements Al and Zr in the alloy system chosen for the manufacture of combustion chambers of the thermal power plants. The phase diagrams of the alloys as well as the solidification diagrams are presented. Also, in this chapter are included the studies of the influences of some alloying elements on the microstructure and properties presented in the specialized literature. The selection criteria for high entropy alloys are presented to help identify the final characteristics of the alloys.

Chapter 3 presents in its first part, the way of obtaining in induction furnace the studied alloys and the heat treatments applied to improve the samples properties. The second part of the chapter presents the physico-chemical characterization of the HEA samples obtained for the two selected applications as well as mechanical tests, plastic deformation and oxidation tests. The influence of the alloying elements on the alloy system intended for the manufacture of combustion chambers in thermal power plants is also studied.

Chapter 4 Concludes the results obtained in the experimental part. It contains comparisons of the results obtained in the thermodynamic modelling process with the results obtained experimentally. It also presents a comparison between the physico-chemical properties of the alloy samples obtained.

Chapter 5 Concludes the results obtained in the experimental part. It contains comparisons of the results obtained in the thermodynamic modelling process with the results obtained experimentally. It also presents a comparison between the physico-chemical properties of the alloy samples obtained. personal contributions to research in the field of high entropy alloys and further research directions are also presented.

At the end of the doctoral thesis are presented the articles and papers published by the author in the field of high entropy alloys and bibliographic sources used in the theoretical study.

Chapter I. Theoretical aspects on high entropy alloys

The first work on high entropy alloys was made in 1981 by Professor Brian Cantor with his student Alain Vincent. They developed several mixtures of echiatomic alloys with different components in equal proportions. It has been observed that only one Fe20Cr20Ni20Mn20Co20 alloy forms a single phase solid solution with FCC type structure. Similar studies on a wider range of alloys were repeated with his student Peter Knight at Oxford University in 1998. He obtained some similar results but also new results were published in a thesis at Oxford.

Professor J.W. Yeh has been independently researching the field of multicomponent alloys since 1995. Based on his own concept of high entropy mixing factor, which plays an important role in reducing the number of phases in such alloys in which advantageous properties are obtained, he supervised the student KH Huang in 1996 to begin research and see the success of the possibility of developing and analysing high entropy alloys. Approximately 40 multicomponent alloys with 5-9 components were made by melting in an electric arc furnace. The microstructure, hardness and corrosion resistance of the cast alloys and the heat-treated ones were investigated. Yeh presented the "HEA concept" in the journal "Advance Engineering Materials" in 2003. In May 2004, the paper "Nanostructured high-entropy alloys with multiprincipal elements — novel alloy design concepts and outcomes" was published, being the first to clarify the concept. by HEA by providing experimental results and relevant theory [1].

Because the combinations of compositions and processes for obtaining high entropy alloys are numerous, and each resulting alloy has unique microstructure and individual properties, to be identified and understood the research work is truly unlimited. It becomes very important to consider the basic concepts of HEA from the very beginning, these including the origin of high entropy, classification, definition, notation, composition and the four basic effects of high entropy alloys.

I.1. Definition of high entropy alloys

Each high entropy alloy consists of several elements, often five or more elements in an equiatomic or almost equiatomic ratio, together with a minor proportion of other elements. The basic principle behind high entropy alloys is that significantly high mixing entropies, favour the stability of solid solution phases to the detriment of intermetallic compounds, especially at high temperatures. This improvement allows them to be easily synthesized, processed, analysed, manipulated and used. In a broad sense, HEAs are defined as alloys containing at least five main alloying elements, each with an atomic percentage of between 5% and 35%. The atomic percentage of each minor alloying element, if any, is therefore less than 5% [2].

The name high entropy alloys (HEA) comes from statistical thermodynamics, where Boltzmann's equation [3, 4] can be used to calculate the configurational entropy of a system:

$$\Delta S_{mix} = k \ln w \tag{I.1}$$

where k is the Boltzmann constant and w is the number of ways in which the available energy can be mixed or divided between the particles of the same system.

Table I.1. Configuration entropies of equiatomic alloys with up to 13 constituent elements [5]

N	1	2	3	4	5	6	7	8	9	10	11	12	13
ΔS_{mix}	0	0,69R	1,1 R	1,39 R	1,61 R	1,79 R	1,95 R	2,08 R	2,2 R	2,3 R	2,4 R	2,49 R	2,57 R

Table I.1 shows the configuration entropies of the equiatomic alloys as a function of the increase of the number of components in relation to the gas constant R. The value of the entropy increases with the increase of the number of constituent elements. According to Richards' rule ΔHf / Tm = ΔSf ~ R, the entropy fluctuation per mole, ΔSf at the transition from solid to liquid phase during melting is about 1R, and the enthalpy change or latent heat per mole, ΔHf, can be approximated as RTm, where Tm represents the melting point temperature. Since ΔHf can be considered as an energy required to destroy about 1/12 of all solid bonds, the mixing entropy of R / mol in a disordered solid solution is large enough to reduce the free mixing energy (Gibbs) ΔGmix , because ΔGmix = ΔHmix-TΔSmix. For example, the value at 1000K is RT = 8.314 kJ / mol. Also, an ideal monoatomic gas has a kinetic energy or an internal energy of 1.5RT. Therefore, the decrease in free energy causes the solid solution phase to have an increased ability to compete with intermetallic compounds, which usually have much lower ΔSmix due to their orderly nature. This means that the tendency of the mixing state of the constituent elements to form will increase with the increasing mixing entropy, especially at high temperatures. It can be seen in Table I.1 and Figure I.1 that the configuration entropy of an echiatomic ternary alloy is already slightly higher than 1R and that of the five-element alloy is higher than 1R by 61%. Moreover, the enthalpy formation of two strongly bonded intermetallic compounds, NiAl and TiAl, divided by melting points, reach values of 1.38R and 2.06R, respectively. Thus, it is appropriate to believe that a ΔSmix with the value of 1R is large enough to resist the ordering of atomic pairs with strong binding energies at high temperatures. Δ 1.5R smix is recommended to be treated as a boundary between high and medium entropy alloys. In addition, 1R is recommended to be the boundary limit for alloys with medium and low entropy, for a mixing entropy lower than 1R is expected to have a lower energy to compete with those strong binding energies. The same similar effects of entropy are to be expected in the case of polymers and ceramics. The large number of components in ceramics and polymers leads to a higher entropy effect of the mixture. Ceramics can be grouped into three categories: low, medium and high entropy ceramics (HEC). Similarly, polymers can also be grouped into three similar categories. In the past, the boundary limits in the field of alloys were set as 0.69 and 1.61R, respectively, and thus the differences in figure 4A are observed. This is because the previous limits are based on the main number of elements, ie 2 and 5 respectively.

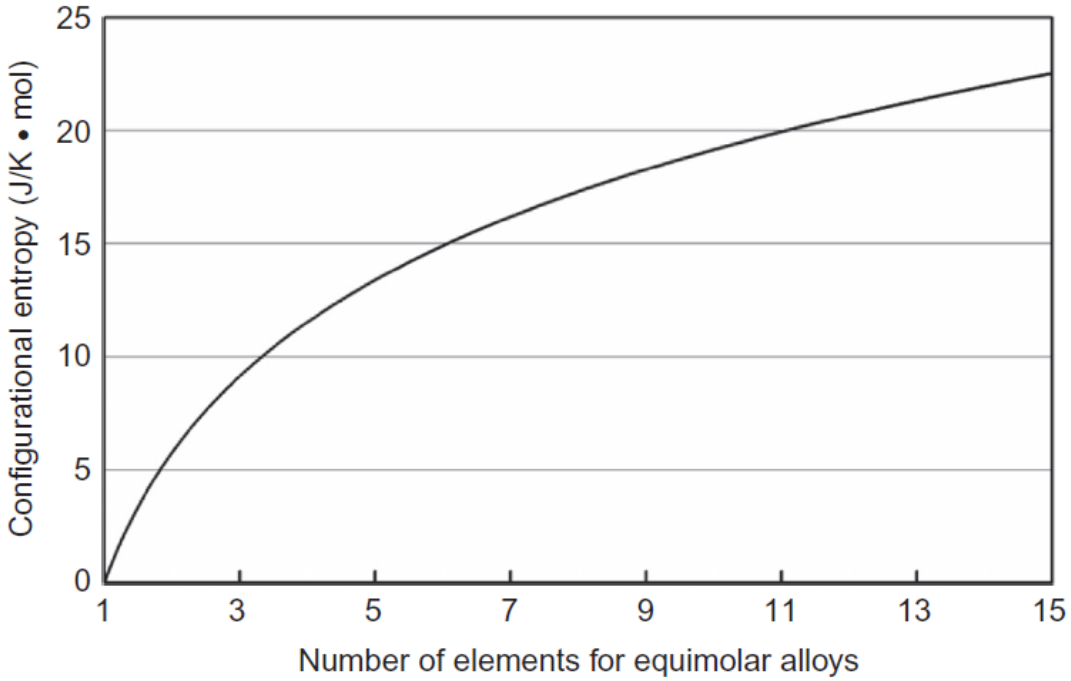

Figure I.1. Configurational mixing entropy according to the number of elements in the equiatomic alloys in the state of disordered solid solution [5].

I.2. Thermodynamic and kinetic considerations

To obtain an alloy with high entropy, a difficult problem is to anticipate the stability of the phases depending on temperature and composition. According to Hume-Ruthery rules, the difference between the dimensions of atoms (δ) and the enthalpy of mixing (ΔHmix) are two dominant factors. For an HEA alloy, the two factors are defined as follows:

$$\delta = \sqrt{\sum_{i=1}^{N} C_i \left(1 - r_i/(\sum_{i=1}^{N} C_i\, r_i)\right)^2} \tag{I.2}$$

$$\Delta H_{mix} = \sum_{i=1, i\neq j}^{N} 4\Delta H_{AB}^{mix}\, c_i c_j \tag{I.3}$$

where r_i is the atomic radius of the i component of the system and ΔH^{mix}_{AB} is the enthalpy of mixing for the binary elements A and B. It is known that the atomic size of an element is affected by the surrounding atoms.

Gibbs law of phase formation determines the degrees of release (F) of a system while maintaining its balance between a number of phases (P) containing a certain number of components (C), under conditions of constant pressure and can be expressed as:

$$P+F = C+1 \tag{I.4}$$

Gibbs law thus shows the maximum number of possible phases in a system with C components in equilibrium. This indicates that condensed systems (systems that do not have a gas phase) cannot have more than C + 1 phases in equilibrium. Thus, binary, ternary, quaternary and five-element systems cannot have more than 3, 4, 5 or 6 equilibrium phases, respectively.

It is important to note that the number of phases observed in HEA alloys is significantly lower than the maximum number of phases anticipated using Gibbs law. This suggests that a large configurational entropy in these types of alloys improves mutual solubility to form solid solution phases (disordered or partially ordered) and thus restricts the formation of a large number of phases. Moreover, the diffusion of atoms is expected to be low and, therefore, the formation of a number of phases is kinetically constrained in such alloys. Thus, the observation of the few phases in HEA alloys is not only due to the high configuration entropy of these alloys, but also due to the low diffusion in these multicomponent alloys. These phenomena are often useful for controlling the microstructure and properties of the material.

I.3. HEA specific effects

There are a lot of factors that affect the microstructure and properties of high entropy alloys. Of these, four basic effects are of major importance. Because HEAs contain at least five elements in major proportions, and conventional alloys are based on one or two major metal elements in proportions, there are differences between the basic effects of the two categories. The specific effects of high entropy alloys are: *the effect of high entropy, severe deformation of the crystal lattice, slow diffusion and the cocktail effect*. In the system thermodynamics, the effect of high entropy can interfere with the formation of complex phases. In terms of the structure, severe deformation of the crystal lattice can greatly alter the characteristics of the alloy. Within the properties, the cocktail effect usually exceeds the quantities anticipated by the mixture, due to the mutual interactions of different atoms and causes the deformation of the crystal lattice.

High entropy effect

The effect of high entropy is of particular importance because it improves the formation mechanism of solid solutions and makes the microstructure much simpler than would be expected. Based on the concepts of physical metallurgy, it is foreseeable that in such alloys many interactions will take place between different atoms of the elements and thus lead to the formation of different types of binary phases, ternary, quaternary compounds, and / or segregated phases. Thus, these alloys would have a complicated structure not only difficult to analyse, but also fragile by nature. This in fact neglects the effect of high mixing entropy.

Since the Gibbs mixing free energy, ΔG_{mix} is $\Delta G_{mix} = \Delta H_{mix} - T\Delta S_{mix}$, where ΔH_{mix} and ΔS_{mix} are enthalpy and entropy of mixing, the high content of elements would decrease the Gibbs free energy, especially at high temperatures contributing to a higher ΔS_{mix}.

In a solid-state alloy, the steady state is that which has the least free mixing energy according to the secondary law of thermodynamics. There are three possible categories of states that compete for equilibrium: elemental phases, intermetallic compounds, and solid solution phases below the melting point. The elementary phase is the terminal solid solution based on a single metallic element. The intermetallic compound is a stoichiometric compound that has a specific crystal lattice, such as NiAl (B2 structure) and Ni3Ti (D024 structure). The solid solution is a phase with complete or significant mixing of all elements in a BCC, FCC or HC structure. Intermetallic phases or intermediate phases based on intermetallic compounds are also

considered solid solutions, but are partially ordered solid solutions [6, 7]. In such phases, the different constituent elements tend to occupy different places in the structure of the crystal lattice.

From the literature analysis it is suggested that at room temperature, ΔSmix in HEA alloys may be sufficient to destabilize 5-10% of intermetallic compounds (those with the lowest enthalpies of formation). An additional 30-55% of the ordered compounds can be suppressed in HEA at a temperature of 1500K. About 50% of intermetallic compounds can be stable at 300K, but unstable at 1500K. It was also pointed out that this effect offers a new approach to the control of microstructure (by dissolving particles and their subsequent controlled precipitation) and the properties of high entropy alloys by hardening particles.

The difference in atomic size between the elements of an HEA alloy also influences the stability of the disordered solid solution phases due to the deformation of the crystal lattice and thus contributes to the potential energy of the enthalpy of mixture and the free energy of Gibbs. On the other hand, there are a variety of structures that form preferentially under the influence of the large atomic size difference.

Severe lattice distortion effect

Because the multicomponent matrix of each solid solution phase in high entropy alloys (HEA) is an entirely solute-type matrix, each atom is surrounded by different other types of atoms and thus the matrix undergoes a deformation of the crystal lattice and due to different atomic size, stresses mainly may occur. The medium crystal lattice exists and can be determined by X-ray diffraction. In addition to the difference in atomic size, the different bonding energies and crystal structure of the elements further influence the deformation of the crystal lattice taking into account neighbouring asymmetric atoms.

Sluggish diffusion effect

In diffusion-controlled phase transformations, the formation of new phases requires the common diffusion of several types of atoms to achieve the division of the composition into HEA. As explained, an HEA contains mainly a disordered solid solution and / or an ordered solid solution. Their matrices could be considered an integral solution. As a result, the diffusion of an atom in a solute matrix would be very different from that in the matrix of a conventional alloy. A vacancy in the solute matrix is actually surrounded by the atoms of the various elements throughout the diffusion process. The slow diffusion and high activation energy in HEA alloys are due to the large variation of the potential energy of the network between its spaces. These abundant spaces can prevent the diffusion of atoms and lead to the effect of slow diffusion.

Sluggish diffusion could affect phase germination, growth and distribution as well as the morphology of a new phase by controlled diffusion phase transformation. It also offers various advantages over the control of microstructure and properties: ease in obtaining supersaturation and fine precipitation, increases recrystallization temperature, decreases grain growth rate,

reduces particle growth rate and increases creep resistance. Therefore, slow diffusion is a generally positive aspect for improving the properties of HEA alloys. For example, fine precipitation and grain structure can improve toughness and strength. Improved creep resistance can extend the life of parts used at high temperatures [8].

Cocktail effect

In alloys with high entropy, the cocktail effect is used to strengthen the properties of at least five major elements. Because the alloy could have a single phase, two phases, three phases or more, depending on the composition and processing, all the properties are due to the contribution of the constituent phases. This refers to the size of the phase in the alloy, the distribution, the limits and the properties of each phase. Moreover, each phase is a solid multicomponent solution that can be viewed as an atomic-scale composite. Its composite properties come not only from the basic characteristics of the elements, but also from the mutual interactions between all the elements, as well as from the effect of excessive deformation of the crystal lattice. The mutual interaction and deformation of the network would bring quantities in excess of those anticipated, by the mixing rule. Overall, the cocktail effect varies from the effect of the multicomponent composite at the atomic scale, to the effect of the multiphase composite at the micro and macro scale.

I.4. Microstructure and phase formation in high entropy alloys

In 1920, Hume-Rothery identified the factors that influence the formation of compounds and the control of the behaviour of the alloy. He identified the link between solubility and factors such as: atomic size, crystal structure, valence and electronegativity of two components in an alloy. Despite the large number of researchers who have tried to address this problem of solubility, the simplicity and generality of Hume Rothery's rules have become one of the most important foundations in materials science [9]. Hume Rothery's rules in a solid solution consisting of two elements are:

1. The difference of the atomic size between solute and solvent shall not exceed 15%. For complete solubility, the difference must be less than 8%.

2. The crystal structures of the two elements must be compatible.

3. Extended solubility occurs when the solvent and solute have the same valence.

4. The two elements should have similar electronegativity to avoid the formation of intermetallic compounds.

The concept of elaborating HEA alloys is based on the principle of configuration entropy given by $\Delta Smix = -R \Sigma Xi \ln Xi$ per mol. Non-equiatomic alloys have a lower configurational entropy because their composition derives from that of equiatomic alloys. This implies that the tendency of solid solution formation would be higher in equiatomic HEA alloys. However, many researchers base their studies on these non-equiatomic alloys. First, the difference between the configurational entropy of equiatomic and non-equiatomic HEA alloys is not very large. For example, the entSmix mixing entropy of the six-component AlCoCrCuFeNi alloy is

1.93R, while the ΔSmix in the Al0.2CoCrCuFeNi alloy is 1.78R. Second, many non-equiatomic HEA alloys exhibited superior mechanical properties corresponding to equiatomic HEA alloys. Thirdly, it is interesting to determine the effect of different alloying elements on the structure and properties of alloys. Yeh [10] studied the effect of aluminium in AlxCoCrCuFeNi cast alloys and showed how the addition of small amounts of aluminium (0.5% at.) in an alloy forms a FCC-type crystalline structure, but as the amount of aluminium increases, it favours the formation of a phase with BCC type structure. This helps to develop HEA alloys with a well-established microstructure and properties.

I.5. Methods for obtaining high entropy alloys

High entropy of the liquid alloy can facilitate the formation of phases with high entropy. However, kinetics plays an important role in the formation of phases. The microstructure of the alloy can be controlled by the cooling rate, the type of processing to which it is subjected and the plastic deformation in combination with different heat treatments. Thus, the properties of the alloy can be optimized by controlling the process parameters.

I.5.1. Induction furnace melting

Electromagnetic induction heating is based on the Joule effect of induced currents due to the penetration of the electromagnetic field into a conductive material located in a time-varying magnetic field. Any electrically conductive body is heated by the Joule effect when it is crossed by an electric current. In the case of electromagnetic induction heating, the conductive material is placed in a time-varying magnetic field, created by a coil crossed by an AC electric current. By introducing a body of conductive material inside the coil crossed by AC current, the variable magnetic flux passing through the material induces electromotive voltages that cause vortices.

Advantages:
• very high temperatures are obtained in the whole mass of the metal melt, as a result of a high concentration of power;
• as a result of the intense mixing (agitation) of the molten metal bath under the action of electrodynamic forces, the temperatures become uniform, local overheating is eliminated and the metal losses are reduced accordingly (0.5 ... 0.8%);
• very pure metals or alloys are obtained, the charge being protected from the chemical action of the electrodes of the arc furnaces, or of the fuel from the flame furnaces; melting is possible in vacuum or controlled atmospheres;
• operating noise has low values, below (70 - 80 dB);
• environmental pollution is very low, the amount of dust being of the order of 0.5 kg / t compared to arc furnaces, where we have 5 - 8 kg / t;
• automatic power adjustment is easy to achieve;
• compared to channel induction furnaces, crucible furnaces have a simpler construction, lower thermal and mechanical stresses and the crucible furnace can be completely emptied after each load;
• Start faster from the cold. The maximum power of the power supply is available instantly, considerably reducing the time required to reach the working temperature;

•Flexibility. A molten metal charge is not required to initiate the start of the melting process, this feature facilitating repeated cold starts and frequent changes in alloy composition;
• Lower need for refractory materials. Due to their compact size and high melting speed, induction furnaces require much fewer refractory materials compared to equipment that uses various fuels.
Disadvantages:
• Slag driving in the batch;
• Strong mechanical stress on the crucible liner, due to the intense agitation of the molten bath;
• High cost due to power supplies (usually generators, if not working with industrial frequency) and the necessary capacitor banks.

I.5.2. Vacuum electric arc furnace

Electric arc vacuum melting has several important characteristics such as: removal of non-metallic inclusions and removal of gases from the melt, high density of the alloy with the desired grain structure and low macro segregation. The high temperature and the low working pressure ($10^{-2} \div 10^{-4}$ torr) facilitate the elimination of the trapped gases in the metallic material, but at the same time favour the appearance of the evaporation process of the elements with high vapor pressure. The structure of the ingot grains obtained by this process consists of columnar-shaped grains for small-diameter ingots or, in the case of large-diameter ingots, a combination of columnar and equiaxial grains. This technique is useful for melting elements with high melting points; however, in the case of elements with low melting temperature and high vapor pressure such as Mg, Zn, Mn, Al, this technique does not provide a very precise control of the composition. For elements with a low melting temperature, an alternative is melting in an electric resistance furnace or in an induction furnace. Also, from an industrial manufacturing perspective, vacuum electric arc furnace is not the best choice due to the limited shape and volume of the melting crucible and the high manufacturing cost [11].

I.5.3. Levitation furnace

The principle of operation of the levitation melting technique is based on the electromagnetic effect. A conductor placed in the high frequency electromagnetic field behaves like a diamagnetic material in the permanent magnetic field. It is pushed to the area where the magnetic field is weakest due to the interaction between the external field and the internally induced currents in the conductor. At the same time, the Eddy currents heat and melt the material. For the levitation phenomenon to occur it is necessary to create a gradient, and the value of the magnetic component of the field to compensate for the weight of the material.

Levitation melting offers many advantages compared to classical techniques. The main advantages are: clean melting environment and high temperatures that this equipment can reach. The molten metal does not come into contact with the walls of the crucible which is the main source of contamination with oxides, carbon or sulphur. The contamination is accentuated by the agitation forces produced by the inductive electromagnetic field. In the case of levitation melting, these agitating forces are beneficial as they produce melting agitation and mixing of alloy components, resulting in a homogeneous ingot of high purity [12].

I.5.4. Mechanical alloying

With the help of this method it is possible to obtain complex materials with superior performances that correspond to the increased exigencies of the modern industry. Mechanical alloying allows the production of composite metal powders, which are particularly difficult or impossible to achieve by other processes. Thus, by this process can be obtained amorphous phases, intermetallic compounds at room temperature, nanocrystalline powders, alloying of immiscible metals or synthesis of carbides or nitrides at low temperatures.

Compared to current manufacturing processes, the mechanical alloy manufacturing process offers the following advantages [13]:

o the possibility of obtaining composite powders with special characteristics, such as:

- very high degree of dispersion of the secondary phases;
- high degree of amorphization; very small granulation (micronic, submicronic or even nanometric);
- a particularly high degree of solubility of the elements, which allows a significant increase in the mutual solubility of the processed elements;

o the powder stores energy, which is used in the sintering process resulting in a decrease in sintering temperatures, compared to the use of powders as such;

o During the process of mechanical alloying, solid state diffusion processes are initiated between the particles of processed material, which allows obtaining at room temperature interstitial products, carbides, nitrides, silicides, etc.

o the presability and sintering properties are improved, by increasing the specific contact surface between the processed elements and activating the diffusion between the elements.

The process of mechanical alloying is influenced by certain factors that play a particularly important role in the manufacture of homogeneous materials. It is known that the properties of ground powder, such as particle size distribution, degree of disorder or amorphization and final stoichiometry, depend on the grinding conditions [14].

I.6. Applications of high entropy alloys

Although many applications currently use conventional alloys, there is always a high demand for high performance materials. There are several criteria that drive the initiative to develop and improve materials: market requirements and competition, research curiosity, miniaturization, multifunctionality, environmental consequences and increased service life. In table I.2. a series of advanced applications are presented where an improvement of the performances of the current materials is necessary:

Table I.2. Applications where it is necessary to improve materials performance [5]

Application	Requested characteristics
Engine materials	Materials with higher resistance to high temperatures, oxidation, hot corrosion, creep are required
Nuclear materials	Materials with high resistance to high temperatures, resistance to radiation
Tool materials	High resistance at room temperature and high temperatures, wear resistance, impact,

	low friction, resistance to corrosion and oxidation
Combustion chambers	High resistance to high temperatures, wear, corrosion and oxidation
Maritime structures	Corrosion and erosion resistance in saline water
Lightweight transportation	Increased specific strength, high hardness, fatigue strength, creep and plastic deformation properties
Functional coatings for shapes and tools	High hardness at high temperatures, corrosion and wear resistance, low coefficient of friction

High entropy alloys have hardening mechanisms with solid solutions that are very different from conventional alloys. HEA alloys usually have high melting points, and the high flow resistance can be maintained up to very high temperatures.

The essential feature of high entropy alloys is their ability to develop high mechanical properties at high temperatures. These properties recommend HEA materials for industrial applications where the severe working conditions are of major importance.

The most used elements in making HEA alloys, due to their properties are: Al, Co, Cr, Fe, Mn and Ni. Aluminium is used for thermal conductivity, malleability, low density and because it forms light but strong alloys with other elements. Cobalt is mainly used for high temperature resistance, hardness and corrosion resistance. Chromium has anti-corrosion effects resistant to high temperatures. Manganese has increased rigidity, wear resistance and hardness. Nickel has a very good resistance to corrosion, a property that is maintained even at very high temperatures.

I.6.1. High entropy alloys for jet engines. State of the art

The jet engine (Figure I.2.) Is one of the essential components of an aircraft, significantly affecting its performance. A relevant example is the achievement of 50% fuel savings in the case of a Boeing 787 aircraft, compared to similar aircraft of previous generations. About half of this savings is due to improvements made to the metal materials used in engine construction. The other half is due to the use of titanium and composite materials in the fuselage and the contribution of improved aerodynamics [15, 16, 17, 18, 19, 20, 21].

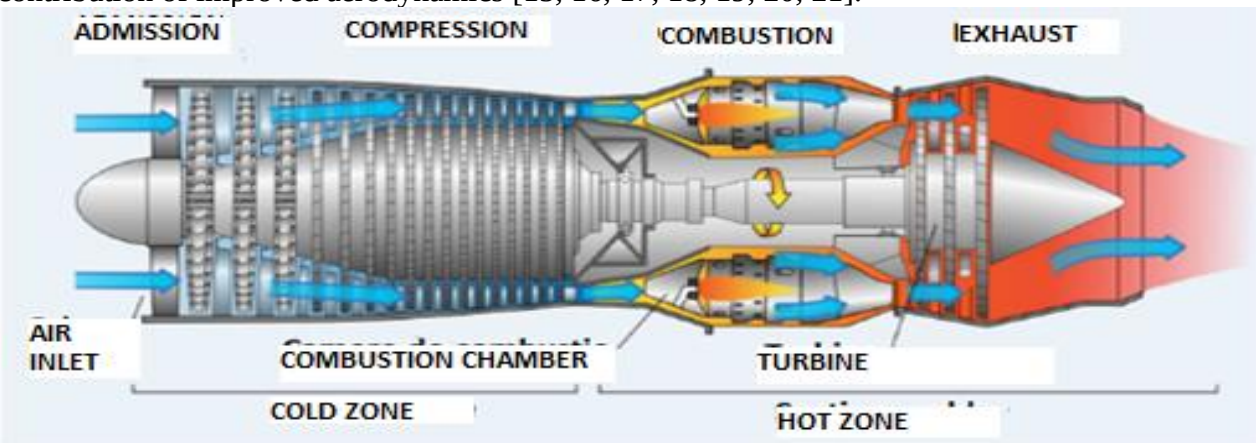

Figure I.2. Principle of jet engine.

High-performance advanced alloys are used to achieve high operating temperatures and a lower weight for modern turbines (Figure I.3).

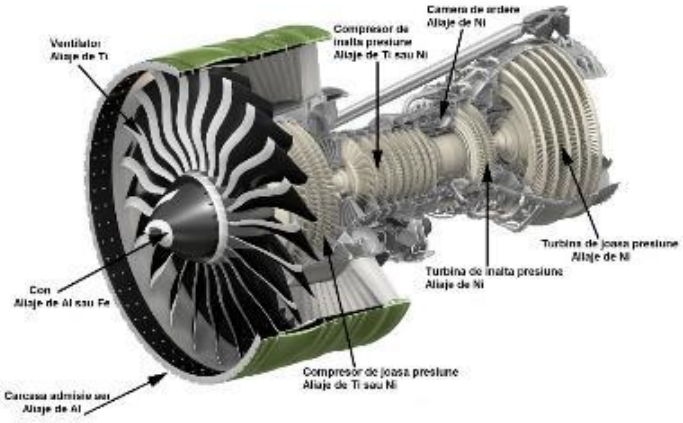

Figure I.3. Currently used materials for jet engines.

Intensive work is currently underway to develop new higher-power engines for aircraft in order to increase their efficiency. The air in the high-pressure compression chamber is compressed even more, leading to an increase in its temperature and the pressure to which it is subjected. In the case of a Rolls Royce Trent CMF Leap X engine, the temperature can exceed 1300 ° C at the end of the compression process. These temperatures far exceed the maximum service temperatures of titanium alloys (600 ° C) and high-alloy steels (450 ° C). At the same time, at temperatures exceeding 600 ° C, the protective oxide layer, which is formed on the surface of titanium components, reacts with oxygen and carbon in the combustion atmosphere, leading to increased hardness and its fragility.

The turbines use as much of the energy of the high-temperature, high-pressure gases leaving the combustion chamber as possible to engage the compressor shaft and to generate electricity for other aircraft components. Given the operating conditions of the turbine, which subject the blades to a very high temperature, a number of measures have been taken to extend their service life, such as the use of materials with high mechanical strength at high temperatures, the design of blades with air cooling ducts or their protection with functional coatings acting as thermal barriers. However, one of the factors that significantly limits the life of turbine blades is fatigue failure, resulting from high dynamic stresses caused by vibrations and resonance during engine operating cycles, which develop speeds in excess of 10,000. of rotations per minute.

Currently, nickel superalloys are used for the sections of the turbine engine at the highest temperatures due to their superior creep and fatigue resistance properties at high temperatures. The most commonly used type of superalloy is INCONEL 718, a precipitation hardened alloy used for high temperature applications [20,21]. It contains significant proportions of Fe, Nb and Mo and minor amounts of Al and Ti. INCONEL 718 combines good chemical corrosion resistance and high mechanical properties with excellent weldability and is widely used in gas turbines, rocket engines, turbine blades and extrusion dies. Ni and Cr contribute to the chemical corrosion resistance of this material. C is also added to precipitate as MC carbides (M = Ti or Nb). Mo is also frequently used as an alloying element in Inconel 718 alloy to increase mechanical strength by hardening with solid solution.

Cobalt-based superalloys are not as strong as nickel-based ones, but retain their mechanical strength up to higher temperatures [16,18]. The ability to retain its mechanical properties at high temperatures is largely due to the distribution of refractory metal carbides (combinations of carbon and metals such as Mo and W), which tend to accumulate at grain

boundaries. This carbide network strengthens the grain boundaries and the alloy becomes stable up to temperatures close to the melting point.
Other materials studied for the production of turbine blades are intermetallic compounds, Mo-Si-B alloys and alloys based on platinum metals [16].

TiAl is considered to be the intermetallic compound with the highest degree of technological maturity for applications in the field of turbine engines. However, its modest melting point (1500 ° C) prevents it from being used at high temperatures and limits it to the low-pressure turbine and static engine components. NiAl has a number of attractive properties for jet engines, such as a high melting point (1650 ° C), good thermal conductivity, low density and good intrinsic oxidation resistance. By alloying with Ta or Cr improved properties of mechanical strength at temperatures higher than 1000 ° C can be obtained. Alloy parts have been successfully made based on this intermetallic through a variety of industrial processes (pressure casting, powder metallurgy, hot extrusion and injection moulding) and tests have already been performed in applications as static parts for stationary turbines.

Mo-Si-B alloys have excellent creep resistance at high temperatures, excellent flow resistance and excellent oxidation resistance at temperatures above 1000 ° C. Their disadvantages include lower oxidation resistance than desired at intermediate temperatures, low fatigue strength, low impact resistance and low breaking strength.

Platinum metal-based alloys (PGM) have excellent oxidation resistance, with low alloying contents. Most alloys have low tensile and flow resistance, very high density and high costs. Ir-based alloys have a very high strength, but no longer possess the oxidation resistance of platinum metal alloys due to the high degree of alloying.

I.6.2. High entropy alloys for combustion chambers. State of the art

Currently, the major global concern is the development of new sources of energy generation with minor influences on the environment (reduction of greenhouse gas emissions) and increased efficiency. This focuses on alternative energy sources (solar, wind, etc.). Although progress has been made in the field of alternative energy generation, the main source of energy remains the burning of fossil fuels. Fossil fuel is the first in Europe but also in the world to generate energy mainly by burning pulverized coal. Today, the production of electricity based on fossil fuels generates over 80% of the planet's needs and is expected to remain the leader with a share of over 50% of energy generation capacity by 2035.

To increase the efficiency of power plants based on burning fossil fuels, the simultaneous increase of pressure and temperature by 4MPa, respectively 30 ° C materializes by increasing the thermal efficiency by about 5 percentage points [22]. This method of growth is burdened by a number of technological restrictions. The main restriction in increasing the initial pressure and temperature is given by the mechanical strength of the thermal circuit components. In the case of using ordinary ferritic steels, the maximum limits are 20 MPa and 570 ° C respectively. The introduction of strong alloy steels of ferritic / martensitic or austenitic type, allows the realization of energy units with supercritical parameters. In this case the pressure can exceed 30MPa and the temperature can reach 600 ° C.

For the combustion chambers of superheaters and reheaters, where the temperature reaches over 650 ° C, materials with high temperatures resistance, good corrosion / oxidation resistance, thermal fatigue resistance and good welding behaviour are required. Martensitic or ferritic steels are often used, but they are limited in terms of high temperature resistance (approximately 590 ℃) and do not have good corrosion resistance in contact with fire or when using sulphur-rich coals. Also, the walls of the coal combustion chambers must have a high hardness and wear resistance at high temperature because by spraying the coals, the walls of

the combustion chamber are subjected to hard contacts with the coal particles. For turbine rotors are used materials such as: forged steels alloyed with CrMoV or 12% Cr, AISI 422SS, steels alloyed with CrMoVWNbN. Superalloys offer an alternative to 12% Cr alloy steels for the manufacture of turbine blades although they are usually used in the case of gas engine turbines [23, 24].

Most Ni-based superalloys have higher creep strength than ferritic alloys by 12% Cr. However, the coefficient of thermal expansion of Ni-based superalloys is generally higher than that of steel by 12% Cr, which considerably reduces the range of suitable superalloys in this case. In addition, superalloys are materials with high manufacturing costs and complex technological processes [25, 26].

Chapter II. Experimental work for designing of high temperature resistant HEA

II.1. Influence of alloying elements on HEA

The most studied alloys with high entropy are based on the CoCrFeNi system to which Al, Ti or Cu are added. The variation of the aluminium content in the alloy causes changes in the microstructure and the crystal lattice. As previously presented in the paper, as the aluminium content increases, the crystalline structure of the alloy transforms from cubic with centered faces into a combination of cubic with centered faces and cubic with centered volume continuing with the complete transformation of the integral crystalline structure into cubic with centered volume [27, 28, 29, 30, 31, 32, 33].

Similar transformations of structures and phases have been observed in other alloys composed of similar systems. A similar alloy system studied contains copper and has been presented in scientific papers by Wu [34], Yeh [27], Tung [35] and Tong [30, 32]. The addition of copper in the system delays the transition of the crystal structure from FCC to BCC, which takes place at an Al1.8 aluminium content. Zhang et al. examined the $CoCrFeNiTiAl_x$ system and obtained the expected results in case of variation of Al content resulting in a transition of FCC structure to BCC. This transition was explained by the packing efficiency of the two crystalline structures, FCCs with a packing efficiency of 74% compared to the packing efficiency of BCC of 68% [33].

Similar studies have been performed on the variation of titanium in the composition of $AlCoCrFeNiTi_x$, $CoCrCuFeNiTi_x$ and $Al_{0.5}CoCrCuFeNiTi_x$ systems [36,37,38]. A study by Zhou et al. [36] shows the effect of variation of Ti content in $AlCoCrFeNiTi_x$ alloy. The presence of titanium in the alloy did not influence the BCC structure of the alloy but it was found the emergence of new phases, including a Laves phase, with increasing Ti content.

Chen et al. [38] studied this alloy system with the addition of $Al_{0.5}$ resulting in $Al_{0.5}CoCrCuFeNiTi_x$. It was found that the crystal structure underwent a single-phase transformation of FCC when x = 0, into a double structure of FCC + BCC and intermetallic structures of Ti when the titanium content increased to x = 2, The atoms packaging efficiency suggest a favouring of the BCC structure in proportion to the increase in large atoms, determined by the low packing efficiency of atoms. This is not the only factor influencing the phase transformation of this alloy. It can be seen that there is still an FCC phase content present when x = 2 and $Al_{0.5}$. This phenomenon suggests that the enthalpies of mixing between the

elements contribute to the stabilization of the phase. With increasing Ti content, ordered and disordered BCC phases and intermetallic phases are formed, which suggests that Ti does not stabilize the BCC phase as Al does. The alloy develops two types of dendritic phases regardless of the Ti content. The composition of the primary dendrites is quite close to the nominal composition, except that Cu is found in a lower proportion [79]. By increasing the content of Ti it is observed how Cu is removed in the interdendritic region. This was attributed to the positive mixing enthalpy that copper has with the other elements in the alloy system, compared to titanium which has a negative mixing enthalpy. This results in favouring the segregation of copper in the interdendritic region and an attraction of titanium in the dendrites.

In high entropy alloys, the increase of titanium content has a hardening effect of the structure but at the same time significantly decreases the ductile properties [36,37]. Similar studies on the ductile properties of $AlCoCrFeNiTi_x$ and $CoCrCuFeNiTi_x$ alloys by Ti content have been published by Zhou [36] and Wang [37].

Studies published in the literature present attempts to produce high entropy alloys using the CoCrFeNi system to which are added various alloying elements such as: Nb, V, Mn, Ag, Au [39,40,41,42,43] . The study of Ma and Zhang [40] shows the influence of Nb on the $AlCoCrFeNiNb_x$ system. At a content of $Nb_{0.1}$, Laves-type phase formations are observed. In this, the formation of a single BCC phase and the Laves phase is observed. The microstructure has a typical dendritic structure with BCC structure and interdendritic regions. As the Nb content increases, the interdendritic region consisting of a BCC phase and a Laves phase also increases [40].

The effect of vanadium content on the microstructure and mechanical properties of the $Al_{0.5}CoCrCuFeNiV_x$ alloy was studied by Chen et al. [43]. The results of the XRD analysis indicate the presence of a phase with FCC structure in the case of V_0 and $V_{0.2}$ which turns into a phase with BCC structure at $V_{0.4}$ content. At a $V_{2.0}$ content, the presence of two phases with FCC structure, respectively BCC, is observed. At the same time, at $V_{0.6}$ - $V_{1.0}$, a third phase of type σ appears, which has the same structure as an equimolar NiCoCr type phase. The maximum hardness of the alloy was measured in the area where the BCC phase is present. When the V content decreased, a decrease in the hardness of the alloy was found. The same hardening mechanism was found by transforming the FCC phase into the BCC phase.

II.2. Specific selection criteria for HEA

According to the latest assessments, the criteria for the formation of simple solid solutions in high entropy alloys contain the following conditions:

- The configural mixing entropy (ΔS_{mix}) must be greater than 11 J / mol · K;
- The mixing enthalpy (ΔH_{mix}) of the alloy must be between -11.6 kJ / mol and 3.2 kJ / mol [44];
- The atomic radius difference criteria (δ), which states that solid solutions are formed mainly for values less than 6.6% and only solid solutions are formed for values less than 4%;
- The derived parameter Ω, which includes the influence of ΔS_{mix} and ΔH_{mix} [45], and which is considered only together with δ. If $\Omega > 1,1$ and $\delta < 3,6\%$ only solid solutions are formed, if $1,1 < \Omega < 10$ and $3,6\% < \delta < 6,6\%$ solid solutions and intermetallic compounds are formed and if $\Omega > 10$ only solid solutions are formed;

- The difference in electronegativity $\Delta\chi$ (after Allen) of the various elements of the alloy must be between 3 and 6% to form only solid solutions;
- The valence electron concentration (VEC-Valence Electron Concentration), which gives indications on the type of solid solution that can be formed: for VEC <6.87 cubic solid solution with centered volume, for 6.87 <VEC <8 mixed structure is formed BCC and FCC, and for VEC> 8 cubic solid solution with centered faces;
- PSFE criterion that expresses the content of elements that can form sigma intermetallic phases. If PSFE> 40% at. the sigma phase is certainly present if 25% at. <PSFE <40% at. it is possible that the sigma phase may not be present in the structure, and if PSFE <20% at. the sigma phase should not be present in the alloy structure. The calculation of PSFE is performed by doubling the atomic percentage of the elements that make up the sigma pairs A50B50. [56,547];
- The influence of the enthalpy of intermetallic compounds formation by calculating the factor k1cr. It must be greater than the value ratio between the enthalpies of the intermetallic compounds formation and those of the mixture to form only solid solutions [48];

II.3. Selection of high temperature resistant HEA using thermodynamic modelling software and specific criteria

For the design of HEA for use in high temperature applications, several aspects have been taken into account that have a strong influence on the final characteristics of the alloys. In order to determine as accurately as possible some high entropy alloy systems and compositions that meet the requirements of the selected applications, the influence of some alloying elements that can be included in the alloy composition but also of some post-processing methods by heat treatments of the samples was investigated in order to improve the physico-chemical and mechanical characteristics.

The starting point for the design of HEA1 and HEA2 alloys was the Cantor FeCrMnNiCo alloy which has been long studied in the literature. It contains elements with useful properties in high temperature applications. Cobalt, which is a critical element and provides low resistance to high temperatures, has been replaced by this composition. Instead, Mo, Nb and W have been added which have the advantages of good oxidation resistance, are refractory elements and form stable solid solutions.

The calculation of HEA specific thermodynamic criteria led to the selection of alloy compositions with specific application properties at high temperatures. Even if the HEA1 and HEA2 alloys have a configural mixing entropy ΔS_{mix} less than 11 J / mol · K this difference is not large. At the same time, for the same compositions, differences of atomic quantities δ were obtained, below the arithmetic mean of the other compositions calculated respectively below 5.85% for HEA1 and below 4.49% for HEA2 which facilitates the formation of only solid solutions. Also, the values of the derived parameter Ω are the lowest results from the calculations. The value of parameter $\Delta\chi$ is the lowest in the case of HEA1 and HEA2 alloys, but not sufficient to be between 3 and 6%. In the case of mixing enthalpy ΔH_{mix} the calculated values for all alloys are in the range of -11kJ / mol and 3.2 kJ / mol. The results of the calculation of the valence electron concentration (VEC) indicate the formation of FCC + BCC type structures in the HEA1 alloy, and in the case of HEA2 it will have a single BCC type

phase. The calculated PSFE criterion of the HEA1 alloy is 55, and for HEA2 it is also 55. The nominal composition of the alloys selected following the calculation of the specific HEA thermodynamic criteria are presented in table II.1.

Table II.1. Nominal composition of selected alloys for jet engines

Alloy	Composition	Elements					
		Cr	Fe	Ni	Nb	Mo	W
HEA1	% gr.	25	25	35	5		10
	% at.	29,44	27,41	36,52	3,29		3,32
HEA2	% gr.	25	25	35		5	10
	% at.	29,47	27,44	36,55		3,19	3,33

Thermodynamic modelling of these alloys was performed using ThermoCalc Pro and MatCalc software. This indicates the formation of equilibrium structures by the presence in large proportion of the ductile phase FCC, even at room temperature. The structure of the alloy has a high number of hard intermetallic phases, but in a small proportion, which in combination with the soft phase FCC can produce an easily workable alloy at room temperature. The alloys have a high melting temperature, which provides high stability at temperatures developed in a jet engine (900-1200 ° C).

The Scheil-Gulliver imbalance diagrams showed, in both alloys, a rapid solidification of the prime range intermetallic phase at a higher proportion than the equilibrium one. Similarly, the solidification of the FCC phase occurs but after the appearance of the gamma prime phase. It is also observed the appearance of an imbalance phase of BCC type, in small proportion at the end of the solidification process. Thus, it is possible that the cast alloy has a higher hardness than the optimized structure at equilibrium due to the higher proportion of the gamma prime phase.

The precipitation of the gamma prime phase was studied with the thermochemical treatment module of the MatCalc software. The results obtained show a faster recrystallization of the gamma phase in the HEA2 alloy, at treatment temperatures up to 800 ° C. At 1000 ° C the absence of the gamma prime precipitate phase is observed for the HEA1 alloy, while the HEA2 alloy has a high value for the proportion of the gamma prime precipitate. This indicates the potential for the development of high mechanical strength properties at high temperatures for the HEA2 alloy.

The alloy system for the manufacture of thermal power plant combustion chamber sheets had as a starting point the same Cantor FeCrMnNiCo alloy as in the case of alloys for turbine blades. Because cobalt has a low resistance to high temperatures, it has been replaced by Al and Zr. Aluminium is used to control the proportion of FCC and BCC phases in the alloy according to Chapter 2.1. Zirconium gives the alloy increased resistance to high temperatures but also better resistance to oxidation at high temperatures.

The calculation of the specific thermodynamic criteria of HEA led to the selection of some alloys that fall within the values of ΔS_{mix} and ΔH_{mix}. The value of the atomic radius difference for the HEA3 alloy suggests the possibility of the appearance of intermetallic compounds, instead for the HEA4 alloy it indicates the predominant formation of solid solutions. The derivative parameter Ω informs about the formation of only solid solutions in both alloys. In contrast, the limit of the value of the electronegativity difference, where only solid solutions can be formed, is exceeded by 1-2% in both alloys. According to VEC in alloys, a duplex of BCC and FCC crystalline structures will be obtained. The calculated value of the

PSFE criterion for the HEA3 alloy is 44 and for the HEA4 alloy is 47. These values indicate a high probability that the sigma phase will be present in these alloys. The nominal alloy compositions selected following the calculation process of the specific HEA criteria are presented in table II.2

Table II.2. Nominal composition of selected alloys combustion chambers

Alloy	Composition	Elements					
		Al	Cr	Fe	Mn	Ni	Zr
HEA3	% gr.	3,26	20,98	22,53	22,16	23,68	7,36
	% at.	6,66	22,22	22,22	22,22	22,22	4,44
HEA4	% gr.	2,28	22,03	23,66	23,27	24,86	3,86
	% at.	4,65	23,25	23,25	23,25	23,25	2,32

Thermodynamic modelling of the equilibrium diagram of HEA3 and HEA4 alloys was performed using MatCalc software. This indicates the formation of FCC and BCC type structures but also of low intermetallic phases. In the case of the HEA3 alloy, the appearance of the prime gamma phase is observed in a low proportion up to the temperature of 750 ℃ but also of an intermetallic phase NiAl which disappears after the temperature of 900 ℃. It is observed the constitution of two cubic phases FCC and BCC respectively. The latter has high proportions at a temperature of about 1100 ℃. According to the equilibrium diagram of the HEA4 alloy, it has a higher melting temperature than the HEA3 alloy, but also a phase ratio with a higher FCC structure, which is maintained in a large proportion up to the temperature of 1150 ℃. The Scheil alloy solidification diagram shows the order of the solidified phases starting with BCC A2 followed by FCC phase A1. The BCC phase A2 solidifies in the HEA3 alloy at 1320 ° and 1310 ° respectively in the HEA4 alloy. The FCC phase A1 solidifies at a temperature of 1090 ° in the HEA3 alloy and 1170 ° in the HEA4 alloy.

Following the modeling of the heat treatment processes at a temperature of 700 ℃, the precipitation of a new phase fraction of sigma type in the HEA3 alloy with low proportions is observed, but also of the NiAl phase. Also, in the case of the HEA4 alloy, the precipitation of a sigma phase is observed, but with higher proportions compared to the HEA3 alloy and also the precipitation of the NiAl phase is observed. Following the modelling of the heat treatment processes at a temperature of 700 ℃, the precipitation of a new phase fraction of sigma type in the HEA3 alloy with low proportions is observed, but also of the NiAl phase. Also, in the case of the HEA4 alloy, the precipitation of a sigma phase is observed, but with higher proportions compared to the HEA3 alloy and also the precipitation of the NiAl phase is observed.

II.4. Modelling the HEA structure depending on the concentration of the alloying elements

For a more precise control of the phases that may occur in the selected alloy systems, modelling was performed using the MatCalc program to determine the influence of the alloying elements added to the Cr-Fe-Mn-Ni system. Because the nickel database was used, some results

could only be obtained under high temperature conditions but could be used to determine a spectrum of possible phases in alloys.

The HEA1 alloy has niobium and tungsten as alloying elements. At room temperature, a concentration of 5% gr. niobium stabilizes a high proportion of γ` phase and a low proportion of Laves phase. At 1000 ℃, the majority of FCC A1 phases and the Laves phase are present. Concentration of 10% gr. tungsten at a temperature of 1000 ℃ leads to the appearance of the majority phase of FCC type A1 and a small proportion of Delta, Laves and BCC A2 phases.

HEA2 alloy has as alloying elements molybdenum 5% gr. and tungsten 10% gr. In the case of molybdenum, at 1000 ℃ it favours the appearance of the majority phase FCC A1 but also the phase with lower proportions γ`. Concentration of 10% gr. tungsten indicates the occurrence of FCC phases A1 and γ`.

HEA3 and HEA4 alloys has aluminium and zirconium as alloying elements. The concentration of aluminium used was chosen taking into account the influence that this element has on the structure of the alloy. In previous chapters it was highlighted that a low concentration of aluminium leads to the formation of an FCC type structure, but at concentration values above the critical limit, it favours the emergence of a duplex of FCC + BCC structures and finally stabilizes the integral BCC structure. Thus, because for the production of power plant sheets it is necessary that the alloy used to have ductile properties, a concentration of 3.26% gr of aluminium was used in the case of HEA3, and then this value was reduced to 2.28% gr. in the case of HEA4 alloy because it was desired to increase the ductile properties of the alloy in the cast state. At these values, the appearance of the two main phases FCC A1 and BCC A2 in close proportions can be noticed.

The concentration of zirconium in the HEA3 and HEA4 alloys was chosen to give the alloy a high hardness, resistance to oxidation at high temperatures but also a good ductility to be processed. Initially, a concentration of 7.36% gr. of zirconium in the HEA3 alloy, but then it was reduced to 3.86% gr. for decreasing the hard phase BCC A2 and increasing the ductile phase FCC A1.

Chapter III. Experimental work for obtaining high temperature resistant HEA

III.1. Experimental research objectives and methodology

Experimental research aims to achieve the main goal of the doctoral thesis by achieving the following specific objectives:

■ Obtaining HEA alloys. Development and casting in vacuum induction furnace of HEA alloy compositions resulted from the modelling processes using ThermoCalc and MatCalc software.

■ Thermodynamic stabilization of the structure and improvement of the physico-chemical characteristics of the alloys.

■ Physico-chemical characterization of the obtained samples.

■ Mechanical testing

III.2. Melting - casting of selected HEA

Melting and casting of HEA was performed in a Linn MFG-30 type induction furnace under vacuum and inert atmosphere. The main characteristics of the induction melting furnace are shown in table III.1.

Table III.1. Features of Linn MFG-30 induction melting furnace

Generator frequency	Generator power	Crucible capacity	Working atmosphere
15 KHz	30 kW	max. 2 litri	- vid 10^{-2}-10^{-3} bar - argon < 1 bar

For the elaboration of the alloys it is necessary to prepare the induction melting furnace in order to ensure the quality of the obtained results. This was done according to the following steps:

1. Checking the condition of the induction melting furnace; 2. Cleaning / degreasing the work area; 3. Preparation of ceramic crucible; 4. Melting / Elaboration of HEA alloy.

For the elaboration of alloys, primary metals were used as raw materials, which were prepared by cutting to dimensions necessary for the composition of the batches and by cleaning - degreasing; were determined by chemical analysis, the compositions of metals introduced into processes. The elaborations were carried out at very high temperatures, of 1550 ÷ 1850°C in a zirconia crucible under vacuum of 10^{-2} bar.

The elaboration experiments were performed in laboratory conditions. The size of the batches was 300g from each type of alloy. The nominal compositions of the alloys are shown in mass concentrations in table III.2.

Table III.2. Nominal composition of selected alloys

Alloy	Composition	Elements								
		Al	Cr	Fe	Mn	Ni	Nb	Zr	Mo	W
HEA1	% gr.		25	25		35	5			10
	% at.		29,44	27,41		36,52	3,29			3,32
HEA2	% gr.		25	25		35			5	10
	% at.		29,47	27,44		36,55			3,19	3,33
HEA3	% gr.	3,26	20,98	22,53	22,16	23,68		7,36		
	% at.	6,66	22,22	22,22	22,22	22,22		4,44		
HEA4	% gr.	2,28	22,03	23,66	23,31	24,86		3,86		
	% at.	4,65	23,25	23,25	23,25	23,25		2,32		

The main parameters of the elaboration / melting process are presented in table 3.3. These are specific to each technological stage: - the melting of the alloy is characterized by the

temperature and the duration of maintenance; - solidification and crystallization are characterized by the cooling rate determined in turn by the chosen mould. After elaboration, the molten alloy was poured into a cylindrical shell of copper or graphite, with the gap footprint of Ø 50mm × 200mm, placed in the vacuum chamber of the furnace.

Table III.3. Melting / casting process parameters

Batch No.	Alloy	Melting/Casting			
		Maintaining temperature, °C	Maintaining time, min	Casting mold	V_{solid},°C/h
1	HEA1	1850	8-10	Copper	10^2
2	HEA2	1850	8-10		10^2
3	HEA3	1550	5-7		10^2
4	HEA4Cu	1550	5-7		10^2
5	HEA4Gr	1550	5-7	Graphite	50

III.3. Improving the characteristics of obtained HEAs by heat treatments

The role of heat treatments is to change the structural and internal stress state of semi-finished products or parts in order to ensure the technical and economic conditions of processing to the final form, as well as the durability and safety requirements in operation of the products.

III.3.1. Influence of heat treatments on HEA

The effect of heat treatments on high entropy alloys and their structural stability at high temperatures have not been studied in great detail. Miracle et al. [49] suggests that long heat treatments at high temperatures are necessary to obtain homogeneous solid solution structures. A study by Zhang et al. [50] on the AlCoCrCuFeNi system highlights the influence of a two-hour heat treatment at 1000 ℃ on the microstructure and mechanical properties of the alloy in the cast state. indicates the presence of a majority phase of the BCC type and a minority phase with the FCC structure in the alloy in the cast state. After the heat treatment, the appearance of a majority phase with FCC structure is observed together with a minority FCC phase. This transformation can be attributed to the high cooling rate when casting the alloy, resulting in a supersaturated BCC structure.

Zhang and Fu [51] studied the effect of heat treatments at 1000 ℃ for 2 hours on the $Al_xCoCrFeNiTi$ alloy. The evolution of the microstructure from the casting stage to the heat treatment stage is materialized by reducing the interdendritic phase in all compositions. The third phase present in the cast alloy, containing $Al_{0.5}$ and $Al_{1.0}$, disappears after the heat treatment process. DRX and EDX analyses reveal similarities in crystal structures and segregation of elements in the interdendritic space [51].

The effect of heat treatment of aging for 4 hours at different temperatures on the hardness of AlCrCuFeNiTi alloy was studied by Pi et al. [52]. According to the DRX analysis,

the structure of the cast alloy has three phases: two BCC phases and an intermetallic phase of the Fe_2Ti type.

III.3.2. Experimental heat treatment works

The heat treatment works for annealing-homogenization of the alloys resulting from the elaboration / casting process took place within the Research-Development Institute for Non-Ferrous and Rare Metals - IMNR, the Laboratory of New Materials and Technologies and within the Institute of Metals and Technology from Ljubljana, Slovenia.

The heat treatment of annealing-homogenization of the alloys took place in an electric furnace, LHT 04/17 Nabertherm GMBH, with controlled atmosphere and maximum working temperature of 1750 ° C and in a low-pressure furnace IPSEN VTTC-324R with temperature maximum working temperature of 1270 ℃.
The stages and parameters of the heat treatment process, corresponding to the technological flow are:
• Charging load for heat treatment
• Enclosure Closure and Vacuum (in case of heat treatments performed under vacuum)
• Heating the sample to the chosen treatment temperature (600 ÷ 1100℃) at a rate of 10℃ / min, under continuous purge of inert gas (argon) or in vacuum.
• Maintain the HEA sample at the desired homogenization temperature (600 ÷ 1100℃) for 10 ÷ 50 hours, under an inert atmosphere of Ar or vacuum.
• Cooling in the oven at room temperature (2℃ / min in an inert atmosphere, 0.5 ℃ / min in vacuum).

Chapter IV. Characterization of obtained HEAs

IV.1. Methods for high entropy alloys characterization

The chemical composition of the resulting alloys was analysed using an ICP-OES device. Optical and electron microscopy (SEM) investigation methods were used to evaluate the microstructure of the alloys. For a better evaluation of the samples, the surface of the samples was attacked with a specific chemical attack solution. The crystalline structure of the constituent phases in the elaborated alloys will be studied with the help of an X-ray diffractometer device. For a better identification of the composition of the alloy phases, the EDS analysis on the surface and in points was also used. For thermal power plants sheets production in order to identify the melting points of alloys and phase transformations at

temperature, the method of differentiated thermal analysis (DTA) and differentiated calorimetry (DSC) was used for the alloys.

IV.2. Characterization of HEA for turbine blades

IV.2.1. Physical – chemical and structural characterization

Chemical and microstructural characterizations were performed for alloys selected from the Ni-Cr-Fe-W-Nb - HEA1, Ni-Cr-Fe-W-Mo - HEA2 systems.

To highlight the homogeneity of the alloy, samples for chemical analysis were taken from various areas of the sample. The results presented in table IV.1. represents the average of these determinations.

Table IV.1. Chemical composition of cast samples

Sample	Chemical composition, % wt.									
	Al	**Cr**	**Fe**	**Mo**	**Nb**	**Ni**	**Ta**	**Ti**	**W**	**Zr**
HEA1	0,067	25	26	0,058	4,12	35,8	0,026	0,038	8	0,026
HEA2	0,063	21	25,5	4,42	<0,005	34,5	<0,005	0,022	9	0,022

Chemical analysis of alloys made by induction indicates a composition close to the nominal one with a few minor differences in concentration. The largest differences were observed in hard-fusible elements such as W, Nb and Mo, which require a high melting temperature and a longer holding time.

The morphological analysis of HEA1 and HEA2 samples melted and casted in induction furnace was studied by optical and electron microscopy (figure IV.1, figure IV.2). They have a large surface dendritic structure and small, well-defined, hard-looking interdendritic spaces. The mapping and punctual EDS analysis on the HEA1 sample indicates the composition of the dendritic phase, which is mostly composed of Cr, Fe and Ni with low Nb and W contents.

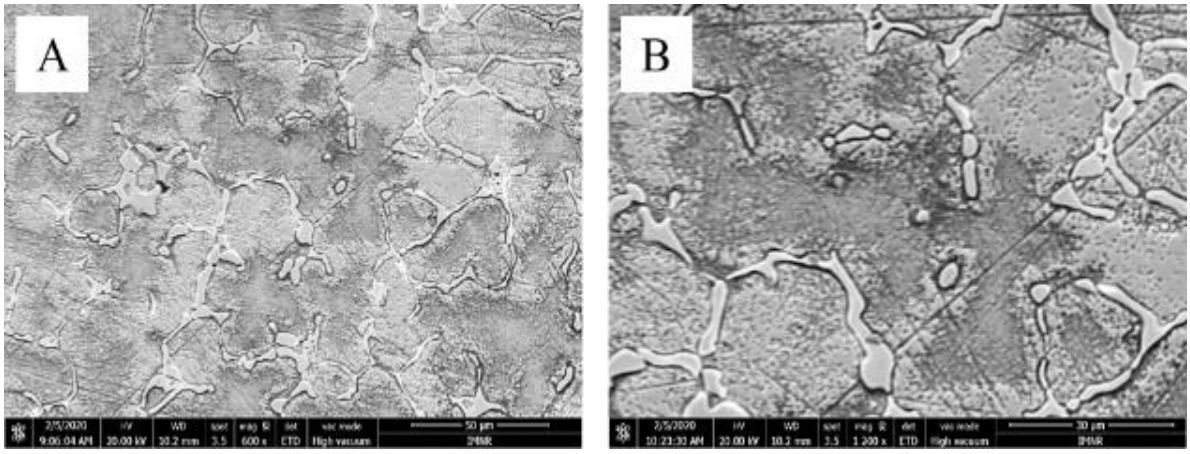

Figure IV.1. SEM analysis of HEA1 alloy. A. magnification 600 ×; B. magnification 1200 ×

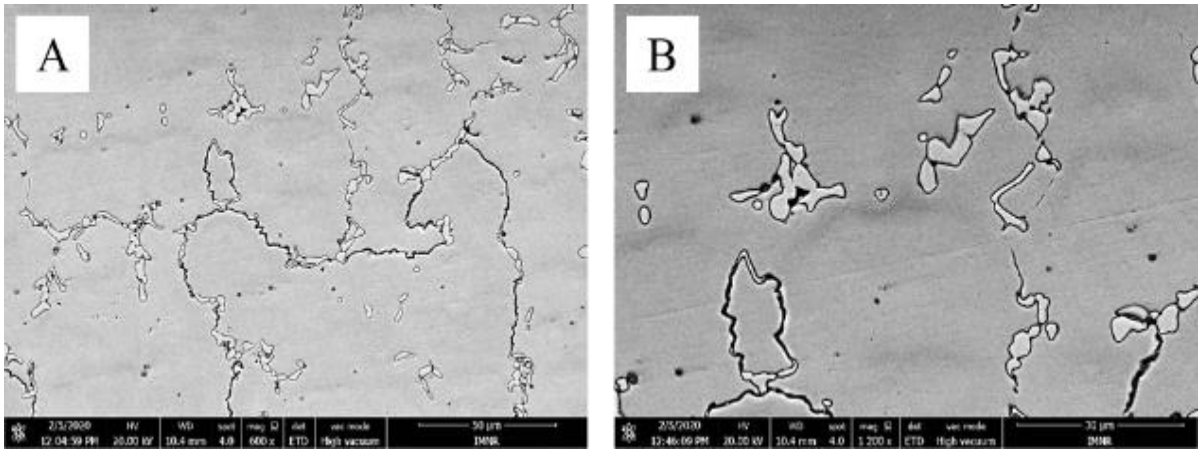

Figure IV.2. SEM analysis of HEA2 alloy. A. magnification 600 ×; B. magnification 1200 ×

According to the point EDS analysis in the interdendritic phase, all the elements present in the alloy are found in similar proportions. However, according to the mapping EDS analysis, the interdendritic phase consists of Nb and W in high proportions. You can also see the presence of tungsten in all noted phases. The EDS analysis of the HEA2 alloy shows a distribution of elements similar to that of the HEA1 alloy. The dendritic phase consists mainly of Cr, Fe, Ni, and in the interdendritic phase are present all the component elements of the alloy, with a low concentration for Mo. Also, the EDS mapping analysis indicates a distribution of tungsten throughout the mass of the alloy but also a homogeneous distribution of chromium in the alloy. Segregations of elements such as Mo, Nb and W in the interdendritic zone may be due to their high melting temperatures and the low holding time at the melting temperature of the alloy during processing.

The results of X-ray analyses (table IV.2) on samples HEA1 and HEA2 indicate the presence of solid solutions typical of high entropy alloys. The HEA1 alloy has a safe solid solution phase A1 with FCC structure. This can be attributed to the high Ni content which favours the appearance of the FCC type structure. HEA2 has an A2 BCC solid solution phase and an A1 FCC solid solution phase. As in the case of HEA1, the appearance of phase A1 with FCC structure is favoured by the high Ni content of the alloy. The appearance of the solid solution phase A2 with BCC structure may be due to the presence of molybdenum.

Table IV.2. Results of X-ray diffraction analysis of HEA1 and HEA2 alloys

Compound	Reference PDF	System	Spatial Group	a
HEA1				
Solid solution A1	00-047-1417	FCC	Fm-3m (225)	3.6133 A
HEA2				
Solid solution A1	00-047-1417	FCC	Fm-3m (225)	3.6022 A
Solid solution A2	04-018-6601	BCC	Im-3m (229)	3.1222 A

IV.2.2. Mechanical characterizations

The hardness of the elaborated alloys was analysed using a Vickers durometer using a force of 2N, an indentation time of 2s and an indentation speed of 0.6 N / s. The results presented in table IV.3 are the arithmetic mean of 3 measurements.

Table IV.3. Hardness of HEA1 and HEA2 alloys before and after vacuum heat treatment

Alloy	Zone	
	Edge	Center
As cast		
HEA1	299 HV	242 HV
HEA2	196 HV	227 HV
Heat treated for 50h at 800°C in vacuum		
HEA1	289 HV	282 HV
HEA2	305 HV	308 HV

The mechanical tests were performed by the partner Institute of Metals and Technology (IMT) from Slovenia within the Mera.Net HEAMODELL project. The test samples were prepared by mechanical turning processes under coolant jet so as not to affect the physical properties of the surface. The threads were also threaded at both ends so that they could be attached to the two ends of the traction device. The results of tensile tests of non-heat treated HEA1 and HEA2 alloy samples are shown in figures IV.3 and IV.4 and tables IV.4 and IV.5. To increase the mechanical properties of the cast alloys, heat treatments were applied at 800 °C for 50 hours. The results of the mechanical tensile tests for the heat-treated samples are shown in figures IV.5 and IV.6 and in tables IV.6 and IV.7.

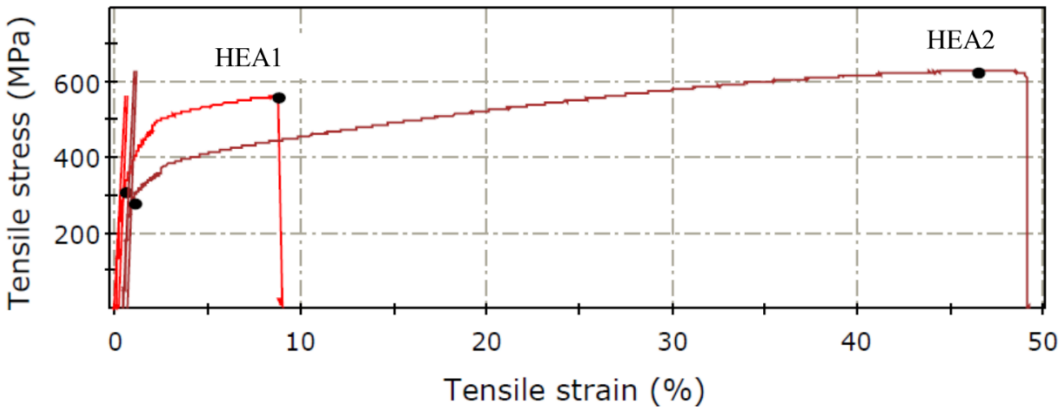

Figure IV.3. Traction stress-strain diagram at room temperature (25°C).

Table IV.4. Tensile test results at room temperature (25°C)

Nr. Crt.	Sample	Diameter (mm)	Area (mm^2)	Yield strength $R_{p0,2}$ (MPa)	Tensile strength R_M (MPa)	Elongation A (%)	Modulus (GPa)
1	HEA1	3,99	12,50	312	561	9,3	107
2	HEA2	3,98	12,44	280	627	37,6	119

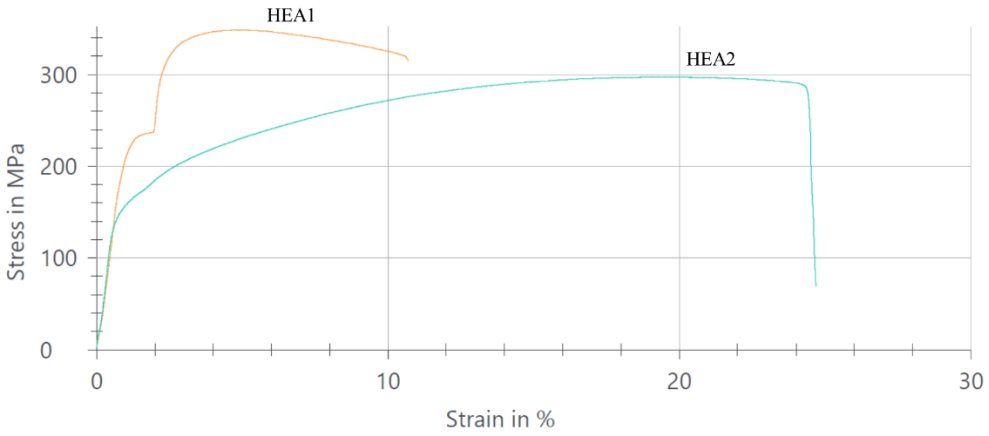

Figure IV.4. Traction stress-strain diagram at room temperature at 800°C

Table IV.5. Tensile test results at room temperature at 800°C

Nr. Crt.	Sample	Diameter (mm)	Area (mm^2)	Yield strength $R_{p0,2}$ (MPa)	Tensile strength R_M (MPa)	Elongation A (%)
1	HEA1	3,97	12,38	216	349	12,3
2	HEA2	3,98	12,44	147	297	28,7

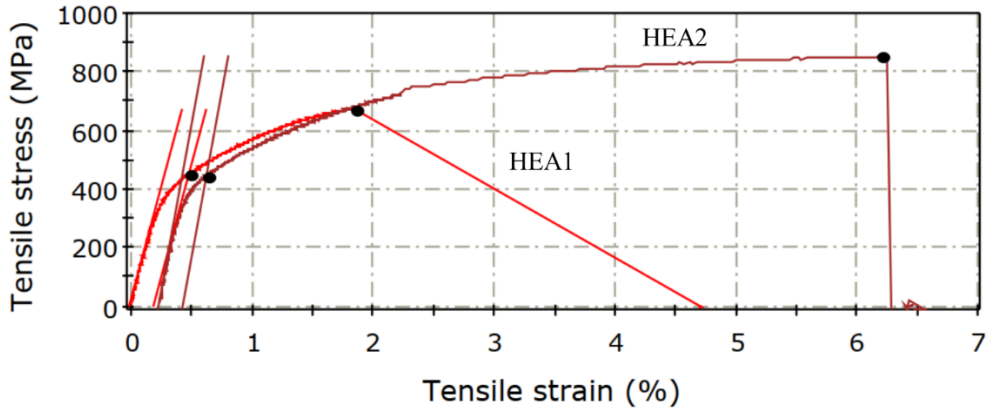

Figura IV.5. Traction stress-strain diagram at room temperature of HEA1 and HEA2 samples after vacuum heat treatment.

Table IV.6. Results of tensile tests at room temperature (25 °C) of samples HEA1 and HEA2 after vacuum heat treatment

Nr. Crt.	Sample	Diameter (mm)	Area (mm^2)	Yield strength $R_{p0,2}$ (MPa)	Tensile strength R_M (MPa)	Elongation A (%)	Modulus (GPa)
1	HEA1	3,97	12,38	450	674	1,8	154
2	HEA2	4,0	12,57	445	852	5,5	228

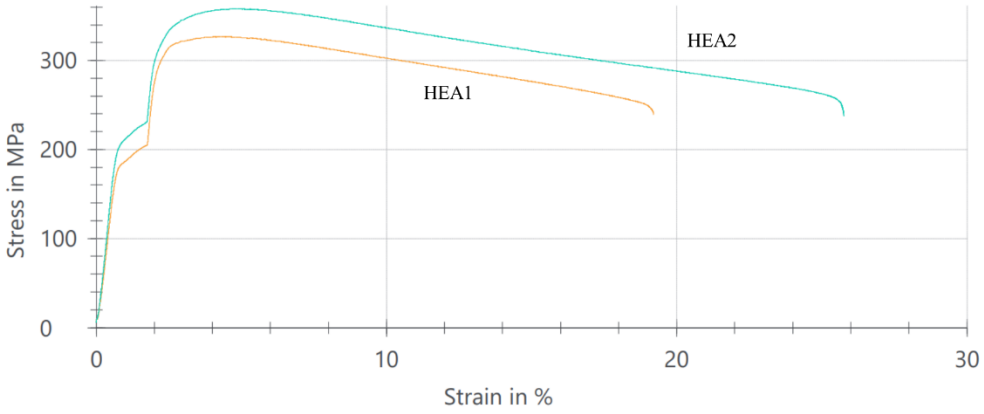

Figure IV.6. Stress-strain diagram at 800 ℃ for vacuum-treated HEA1 and HEA2 alloys

Table IV.7. Results of the tensile test at 800 ℃ for heat treated HEA1 and HEA2 samples

Nr. Crt	Sample	Area (mm^2)	Yield strenght $R_{p0,2}$ (MPa)	Tensile strenght R_M (MPa)	Elongation A (%)
1	HEA1	12,44	184	327	24,1
2	HEA2	12,55	207	358	32,7

It can be seen that the heat-treated samples have a higher mechanical strength compared to the untreated ones, both the flow value and the breaking value. The mechanical strength of the alloys remains high at 800 ℃. The elongation of the HEA1 alloy is considerably smaller than that of the HEA2 alloy in untreated samples. After heat treatment the relative elongations of the alloys are considerably closer. At the working temperature of 800 ℃, the relative elongation of the samples increases as expected, which will also improve the creep resistance. Surprisingly, the relative elongation of the HEA1 alloy is superior to the HEA2 alloy given that the HEA2 alloy has a higher mechanical strength.

IV.3. Characterization of HEA developed for combustion chambers

IV.3.1. Physical – chemical and structural characterization

After melting in induction furnace the alloys HEA3, HEA4, HEA4Cu and HEA4Gr, compact ingots were obtained from which samples were taken from the 3 areas (base, middle area and upper area) to be chemically analysed. The result of the chemical analyses (Table IV.8) showed a relatively homogeneous distribution in the entire volume of the ingots. Following the remelting of the HEA3 alloy, the HEA3R sample was obtained in which the distribution of elements such as: Fe, Ni, Zr was standardized, getting closer to the nominal composition of the alloy.

Tabelul IV.8. Chemical composition of the alloys obtained (average of the 3 chemically examined areas)

Alloy	State	Al	Cr	Fe	Mn	Ni	Zr	Cast mould
HEA3	As cast	3,72	20,35	23,47	21,41	22,39	6,24	Copper
HEA3R	Remelted	3,98	21,70	22,42	22,07	23,11	6,44	
HEA4Cu	As cast	2,53	22	23,88	23,66	24,89	3,02	
HEA4Gr	As cast	2,52	21,17	23,71	23,37	25,61	3,60	Graphite

The microscopic study of the casted samples and attacked with a solution of HF, HNO3 and H2O, highlights the presence of dendritic structures typical of these alloys with interdendritic areas in which the eutectic formed by solid solutions is present. It is also observed the appearance of a hard compound with micron dimensions appeared in the first phase of crystallization,

Comparing the as cast HEA3 alloy with the HEA3R alloy (remelted HEA3) it can be seen that the elongated dendrites with relatively short lateral arms have reduced their size, thus increasing the interdendritic areas. In the microstructure of HEA4Cu and HEA4Gr alloys that had different cooling conditions, there are differences in the proportion of the dendritic phase, but also in its shape. Due to the higher cooling rate of the HEA4Cu alloy, it has a smaller dendritic structure, slightly oriented and large secondary arms.

The SEM analysis of the casted samples is presented in figure IV.7. The presence of two main phases in the HEA3, HEA3R alloys and the presence of three main phases in the HEA4Cu alloys can be observed and in the HEA4Gr sample the interdendritic area is made up of two phases. Also, in the HEA3 sample can be seen the presence of hard formations that are identified by EDS analysis as Zr-based compounds.

The application of heat treatments on HEA3, HEA4Cu and HEA4Gr alloys (figure IV.8) led to a refining process of the structure through which the dendritic areas and also the interdendritic ones were diminished. Thus, the hardness of the alloys increased significantly according to the results of the hardness analyses in table IV.10. Figure IV.9 highlights the morphology of the heat-treated HEA3Cu and HEA3Gr samples at 700 °C for 20 hours. The SEM analysis indicates a decrease, a refinement of the dendritic and interdendritic regions but also a change in the proportions of the two interdendritic phases.

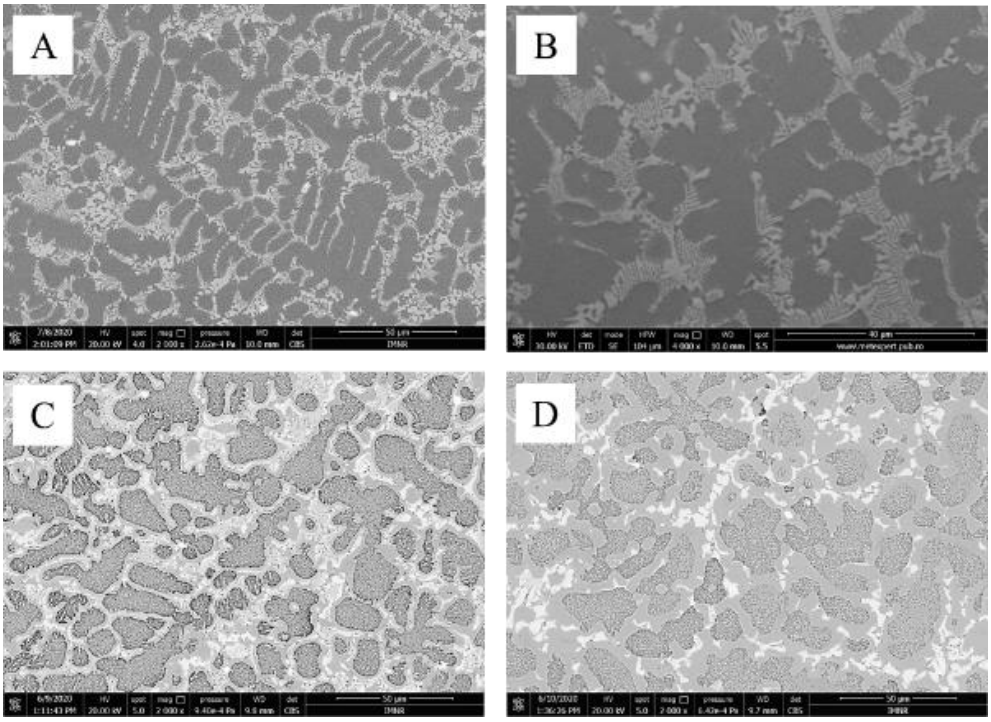

Figure IV.7. SEM analysis of cast alloys. A. HEA3; B. HEA3R; C. HEA4Gr; D. HEA4Cu

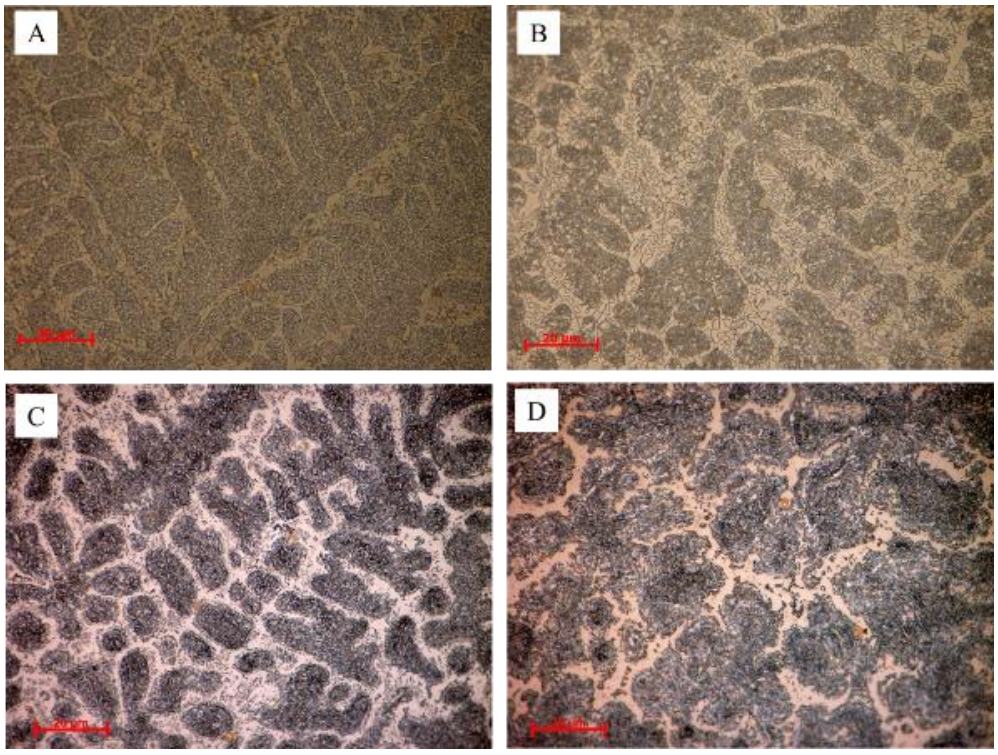

Figure IV.8. Optical microscopy analysis for HEA3 and HEA4Cu / Gr alloys after the heat treatment process. A - HEA3 treated for 50 hours at 700 °, B - HEA3 treated for 50 hours at 800 °, C - HEA4Gr treated for 20 hours at 700°C, D - HEA4 with treatment for 20 hours at 700°C.

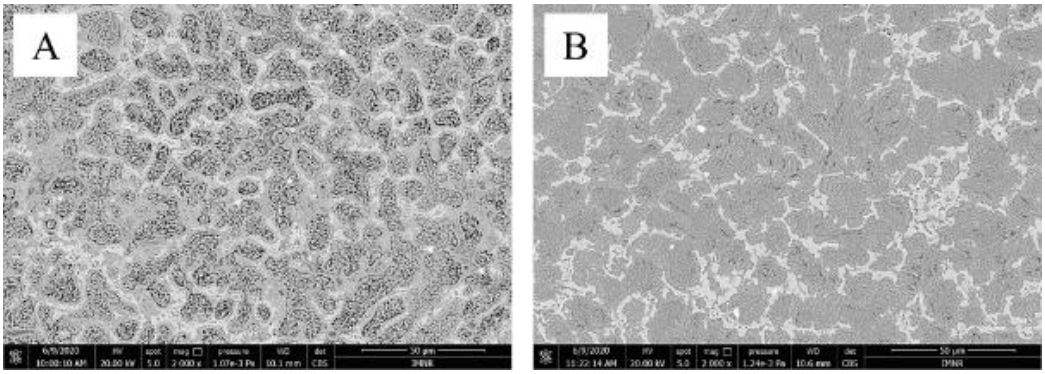

Figure IV.9. SEM analysis of heat-treated alloys for 20 hours at 700 ℃. A. HEA3Gr; B. HEA3Cu.

According to the mapping EDS analysis, in the HEA3 alloy the dendritic region is predominantly composed of Fe, Cr, Mn and Zr, Al and Ni are mainly found in the interdendritic area together with small amounts of Mn. After the remelting process, the distribution of the elements changes by redistributing large amounts of Ni in the interdendritic region and by decreasing the proportion of Al according to the point EDS analysis. Also, the presence of hard Zr compounds is diminished after the remelting process. According to the SEM analysis and the punctual EDS analysis, the interdendritic region consists of two distinct phases with majority contents of Zr, Mn, Ni and Cr, Fe, Mn and Ni, respectively.

Table IV.9. X-ray diffractometry results on HEA alloy samples

Alloy sample	Compound	Content (%)	Lattice parameter (Å)	Crystallite size (nm)
HEA3	Solid solution A2	68	2,88	17
	Solid solution C15	23	6,88	16
	Solid solution A12	9	8,9	15
HEA4Cu	Solid solution A1	63	3,64	14
	Solid solution A2	29	2,89	17
	Solid solution C15	8	6,91	14
HEA4Gr	Solid solution A1	52	3,63	14
	Solid solution A2	36	2,88	17
	Solid solution C15	12	6,90	15
HEA3 TT 20h/700℃	Solid solution A2	25	2,909	29
	Solid solution sigma	48	8,811	46
	Solid solution C15	27	6,872	26
HEA4Cu TT 20h/700℃	Solid solution A2	26	-	-
	Solid solution sigma	67	-	-
	Solid solution C15	7	-	-
HEA4Gr TT 20h/700℃	Solid solution A2	31	-	-
	Solid solution sigma	62	-	-
	Solid solution C15	7	-	-
HEA3 TT 50h/700℃	Solid solution A2	7	2,911	29
	Solid solution sigma	56	8,815	55
	Solid solution C15	37	6,874	39

The constituent phases of the alloys studied for applications in thermal power plants resulting from the DRX analysis are presented in table IV.9. The results of the XRD analysis are partially consistent with those obtained in Chapter 2.3. The analysis indicates the presence of solid solution phases type A1 - FCC, A2 - BCC, phases with cubic structure type Laves C15 and sigma phase. There are major differences in the proportions of phases A1 and A2 in the HEA3Cu and HEA3Gr alloys due to different cooling rates. Thus, phase A2 with BCC crystalline structure is present in higher content in HEA4Gr alloy, which favourably influences its hardness value. This hardening effect is also observed in the HEA3 alloy which has a content of approximately 68% of phase A2 and its hardness is 558HV. After correlating the results of the DRX analysis with the EDS, it can be stated that phase A1 is present interdendritically, phase A2 is present dendritically, phase A12 is present interdendritically in small quantities in HEA3 alloy, phase C15 is present interdendritically in small quantities, and sigma phase appears after heat treatments instead of the FCC A1 phase. Phase C15 is mainly composed of Zr and Ni but also small contents of Mn. The sigma phase that occurs after heat treatments helps to increase the hardness of the alloys according to the hardness tests. It can be identified inside the dendrites due to the high concentration of Cr and Fe but also the presence of manganese.

DTA analysis for the HEA3 alloy (figure IV.10.a) revealed the presence of several peaks up to a temperature of 1100 ° C. The first tip shows the removal of moisture from the sample. The two peaks in the range of 200-300°C are characteristic of abrupt changes in the composition of intermetallic phases such as gamma prime and Ni7Me. Between 600-700°C, a phase transformation from sigma (intermetallic phase) to cubic solid solutions with centered volume (BCC-A2) and cubic with centered faces (FCC-A1) occurs. Around 1000 ° C the NiAl and FCC-A1 phases turn into BCC-A2, which will be predominant in the system.

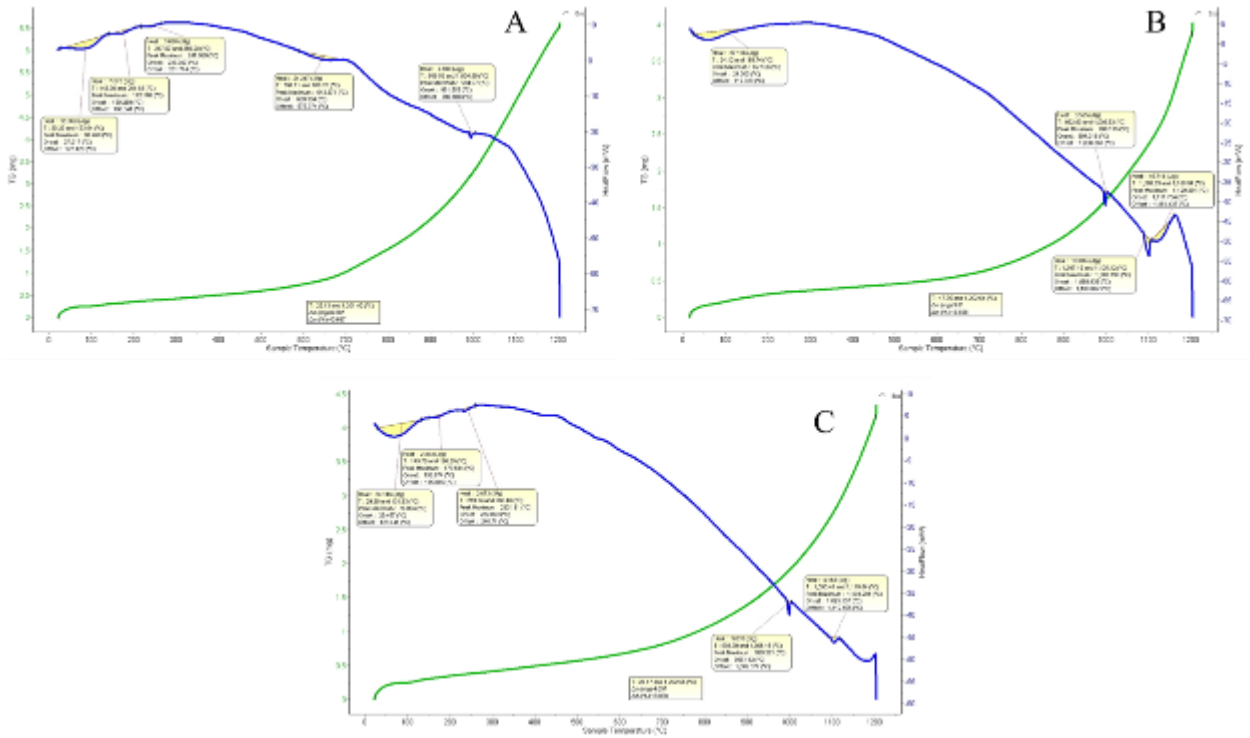

Figure 3.10. Thermal analysis of cast alloys. A - HEA3; B - HEA4Cu; C - HEA4Gr.

The cast HEA4 alloy in the form of copper or graphite shows similar curves on DTA analysis (Figures IV.10.b and c). The major difference is the melting of the alloys, where the sample cast in the form of copper has a much higher peak due to the low thermodynamic stability of the alloy structure. Similar to the HEA3 sample, both curves show the starting peaks, characteristic of moisture removal. The graphite sample (Figure IV.10.c) shows two accentuated peaks in the range of 200-300 ℃, which correspond to the formation of the FCC-A1 and NiAl phases. At around 1000 ℃, both curves show a peak characteristic of the transformation from FCC-A1 to BCC-A2.

The heat treatment applied to the samples of the studied alloys increased the hardness by a percentage between 50-100%. The maximum value reached at indentation was 1022HV in the case of HEA3 alloy for the treated samples for 20 hours and 50 hours at a temperature of 700 ° C, respectively.

The measured values of the hardness of the prepared alloys are presented in table IV.10 and are the arithmetic mean of 3 measurements.

Table IV.10. Hardness tests results as an average between the 3 indentations / sample

HEA3		
Heat treatment temperature	**HT duration**	**Final Hardness**
Ascast		558,1 HV
Remelted		569,9 HV
700°C	10 hours	926,9 HV
	20 hours	1005,6 HV
	50 hours	1022,3 HV
800°C	20 hours	932,2 HV
	50 hours	841,8 HV
900°C	20 hours	929,1 HV
1100°C		369 HV
HEA4Cu		
Ascast		358,2 HV
700°C	20 hours	809 HV
HEA4Gr		
Ascast		388,4 HV
700°C	20 hours	802,4 HV

The hardness value of the HEA3R sample together with the SEM analysis confirms the positive effect that the remelting process has, by incorporating in the present structures the hard Zr compounds. The hardnesses of HEA4Cu and HEA4Gr alloys in the casted state, but also after the heat treatment of 20 hours at a temperature of 700 ℃, are close in value but not as high compared to the HEA3 sample. This difference can be attributed to the decrease in Al content which influences the BCC type hard phase content. Also, the decrease in Zr content contributes to the decrease in the hardness of the alloy. However, the decrease in Zr content also automatically influences the resistance of the alloy to high temperatures.

Following the heat treatment experiments, the behaviour of the HEA3 alloy at different temperatures was observed. The hardness of the alloy has an increasing trend in time during the heat treatment at 700 ℃, reaching a hardness of 1022HV. At a temperature of 800 ℃ the hardness increases after a treatment of 20 hours to the value of 932HV, but it acquires a decreasing trend after a heat treatment of 50 hours, and the measured value was 841HV. Figure IV.11 indicates the optimal heat treatment to increase the hardness as that of 50 hours at a temperature of 700 ℃.

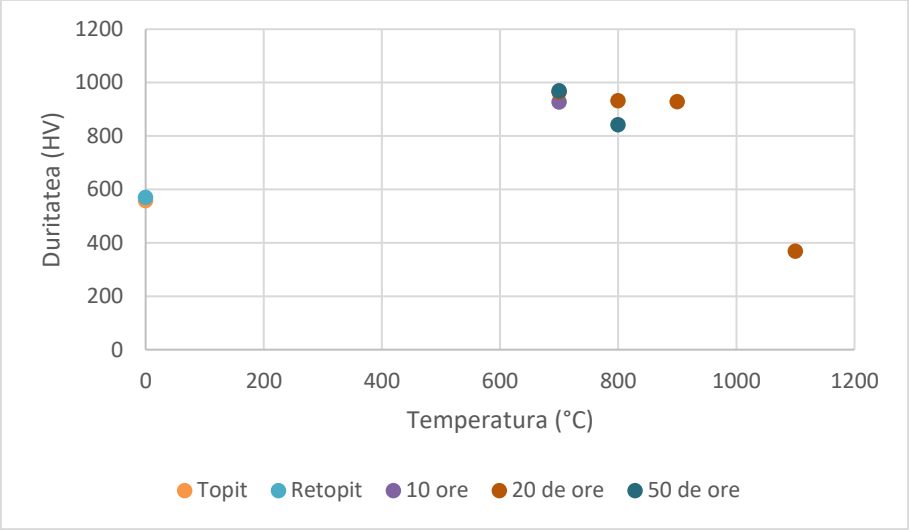

Figure IV.11. Measured hardnesses of HEA3 alloy after different heat treatments

IV.3.2. Mechanical characterization for plastic deformation

The HEA4 alloy was melted and casted in copper or graphite form in a vacuum induction furnace. After cooling, the cylindrical ingot was sliced with an abrasive disk for semi-elliptical sampling. One sample from each batch was plastically deformed with a Mario de Maio rolling mill model LQR 92, reversible quattro.

The rolling process took place gradually, after each passage of the rolled sample between the drums of the rolling mill, the distance between them was reduced by 0.5mm.
Because HEA-type alloys have a high hardness, the deformed samples were preheated to a temperature of 650 ° C. This heating has the role of softening the structure of the alloy and promotes the deformation process, helping to maintain the integrity of the sample subjected to the rolling process. Also, for detailed studies on the ductile properties of the elaborated alloy, 2 samples were hot forged (650 ° C) using a 100TF hydraulic press.

The process of rolling the sample, casted in the copper form, reduced the height of the sample by about 13.5% and in the case of the sample casted in the graphite form, by about 11.5%. The rolling process did not completely deform the part, but only on its x and y axes, but on the faces of the rolled samples appeared deep cracks that increased with each passing of the samples through the rolling mill.
Forging has further reduced the height of the samples compared to the rolling process. Thus, in the case of the copper alloy cast sample, the height was reduced by approximately 49.3%, and in the case of the graphite cast and cooled sample, the height was reduced by approximately 24%. However, the hot forging process also affected the other dimensions of the samples, the surfaces having large differences before and after the forging process.

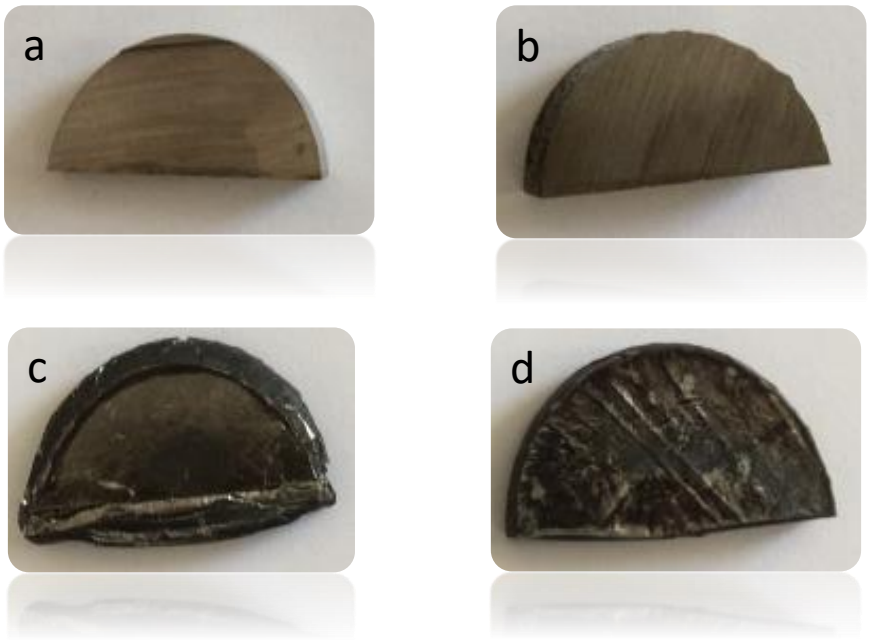

Figure IV.12. HEA4Cu and HEA4Gr before and after forging
A –HEA4Cu; B – HEA4Gr; C – HEA4Cu forged; D – HEA4Gr forged.

Table IV.11. Hardness of alloys after the plastic deformation process

Alloy	Deformation process	Hardness
HEA4Cu	Rolling	419 HV
	Forging	433 HV
HEA4Gr	Rolling	432 HV
	Forging	486 HV

The microstructural analysis after the rolling process indicates a slightly more finished dendritic structure compared to the one resulting from the melting-casting process, with a slight elongation and orientation of the dendrites in the direction of the rolling direction. In the case of samples of plastically deformed alloy by forging HEA4Cu and HEA4Gr, a slight increase in volume of dendrites is observed, but also an elongation of them in the case of HEA4Cu alloy. There is also an increase in the hardness of the samples after plastic deformation, which shows the presence of the hardening state (Table IV.11).

IV.3.3. Characterization of oxidation resistance

For the preliminary testing of the oxidation resistance at high temperatures, the alloy samples intended for the manufacture of the combustion chambers of the thermal power plants were heat treated for 30 hours in the Navertherm LHT 04/17 furnace at a temperature of 700 ℃ in the room atmosphere. The samples were cut in a triangular shape of different sizes with surfaces between 2.33 and 6.08 cm2. They were finished with SiC-based abrasive paper and cleaned in an ultrasonic bath in acetone. The heating rate of the oven was 20 ℃ / min and the cooling was performed in the oven at a speed of about 2 ℃ / min. The evaluation of the oxidation resistance was performed by measuring the mass variation of the samples following

the heat treatment, after a cleaning with a wire brush. The mass of the samples was determined with an analytical balance type OHAUS model Adventure Pro with a detection limit of up to four decimal places (10-4 grams).

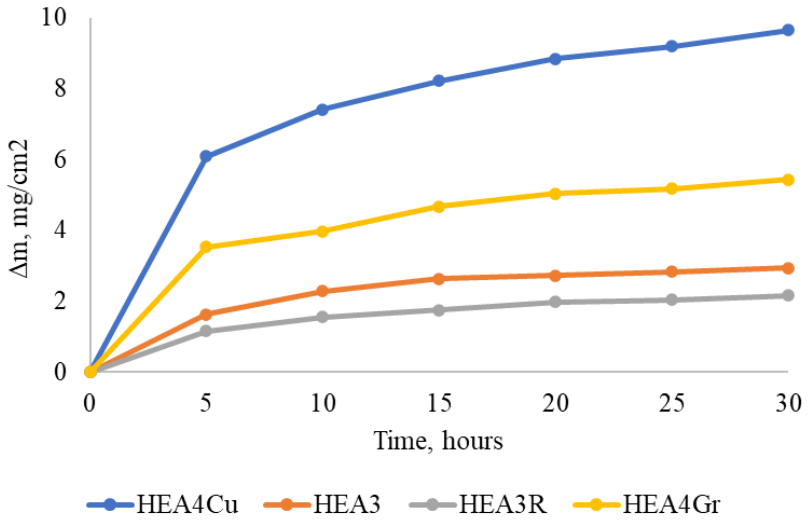

Figura IV.13. Mass loss after oxidation processes

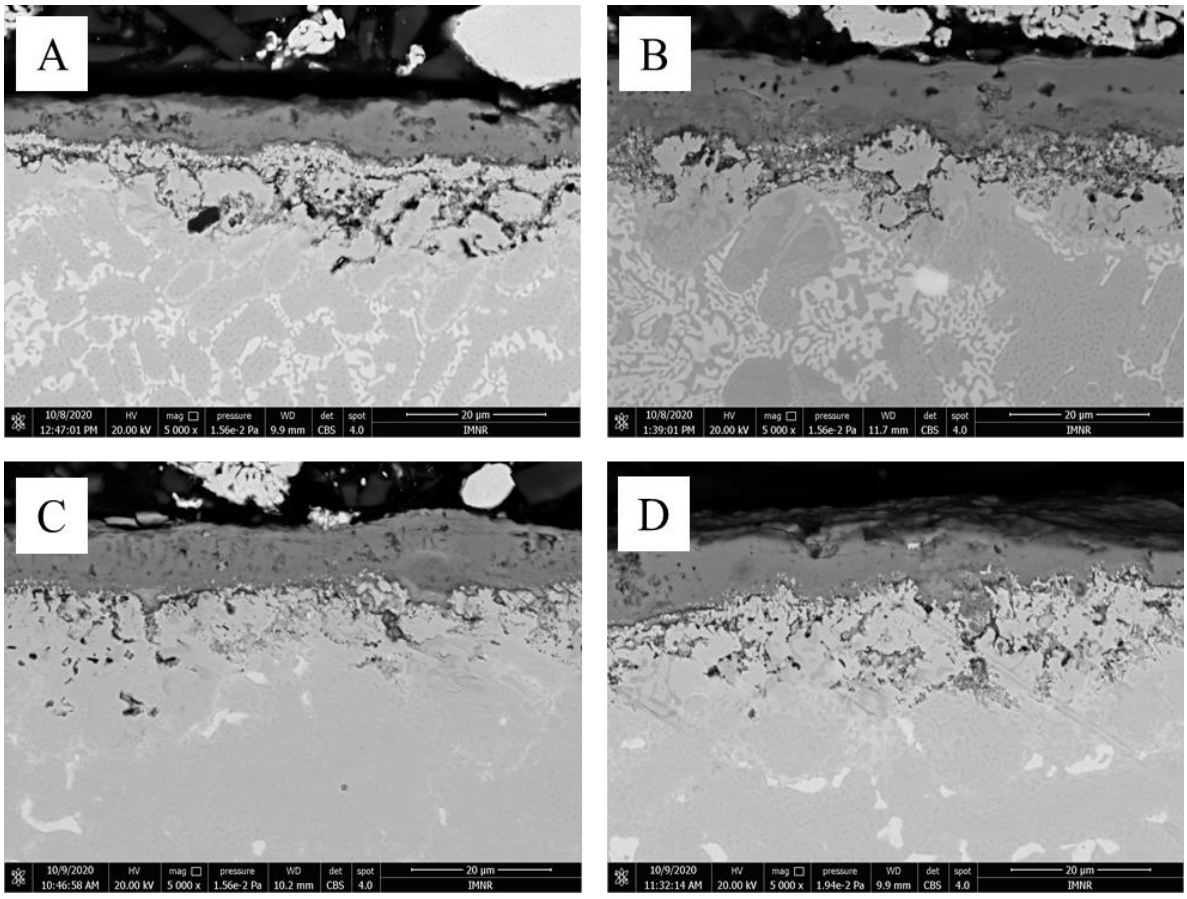

Figura IV.14. SEM analysis of HEA samples after oxidation tests for 30 hours in air
A – HEA3; B – HEA3R; C – HEA4Cu; D – HEA4Gr

The analysis of the oxide layer formed was performed by SEM and EDS (figures IV.14 - IV.15). A high density of manganese can be observed in the oxide area and a high proportion of Al in the immediately following area in the alloy mass. It is also observed the penetration of oxidation in the interdendritic area in the four alloys, more accentuated in the case of the HEA4Gr alloy. To determine the thickness of the oxide layer formed as a result of the heat treatment, 10 measurements were performed on the entire surface of the samples. The average of these measurements are presented in table IV.12. A correlation is observed between the thickness of the oxide layer and the gravimetric analysis of the mass loss. The thinner oxide layer formed in the case of HEA3 and HEA3R alloys can be determined by the higher Al and Zr content in the mass of these alloys.

Tabelul IV.12. Oxide layer thickness of tested samples

Sample	Thickness, µm
HEA3	7,5972
HEA3R	7,4398
HEA4Cu	11,9078
HEA4Gr	9,993

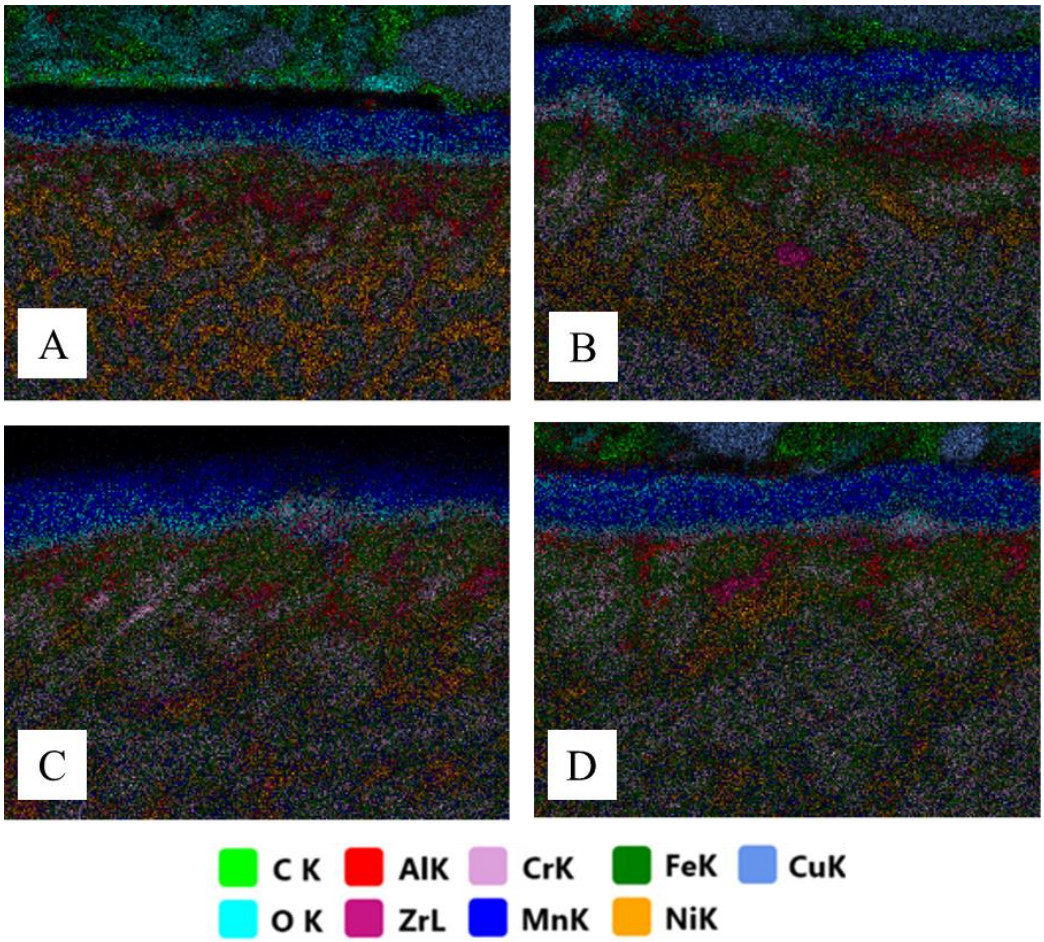

Figura IV.15. EDS mapping analysis of HEA samples after oxidation tests for 30 hours in air
A – HEA3; B – HEA3R; C – HEA4Cu; D – HEA4Gr

Chapter V. Conclusions. Personal contributions. Further research perspectives

Conclusions

- Alloying elements have special importance on the properties of high entropy alloys. The elements often used in practice are: Al, Cr, Fe, Ni and Co. The elements added to increase the mechanical and oxidation resistance, as well as the melting temperature are: Ti, Zr, Ta, Nb, Mo, W. Also, maintaining a low density is very important in aeronautical applications.
- The study of Cr-Fe-Ni-Nb-W - HEA1, Cr-Fe-Ni-Mo-W - HEA2 and Al-Cr-Fe-Ni-Zr - HEA3 / HEA4 alloys, using thermodynamic and kinetic criteria, highlighted their high entropy character, with potential for the formation of mixed complex structures based on solid solutions (cubic with centred volume) and intermetallic compounds.
- The modelling process of HEA1 and HEA2 alloys correctly anticipated the phases following the casting process (FCC A1 and BCC A2). Regarding the HEA3 and HEA4 alloys, the modelling process anticipated the formation of the FCC A1, BCC A2 and Sigma phases in the alloys.
- The mechanical breaking strength of HEA1 and HEA2 alloys was increased after vacuum heat treatment at 800 ℃ for 50 hours. This increased at room temperature by about 20.14% for the HEA1 alloy and 35.88% for the HEA2 alloy. The mechanical strength at 800 ℃ decreased by 6.3% for the HEA1 alloy and increased by 20.53% for the HEA2 alloy.
- Although the alloys were obtained by melting in an induction furnace, a specific process for obtaining homogeneous compositions, the chemical analyzes performed by ICP-OS show the need for the process of melting the alloy. The remelted alloys have a superior chemical homogeneity.
- At the same time, the optical and electron microscopy performed on the cast and fused alloys reveals an advanced finishing of the structure of the fused alloys as well as a uniform distribution of the component phases in the alloy volume.
- Regarding the hardness of the alloys, The best results were obtained after heat treatments. The maximum value is 1022 HV for the heat-treated HEA3 alloy at 700 ° C for 50 hours. The hardness of 1005 HV was also obtained in the case of the HEA3 alloy treated at a temperature of 700 ° C for 20 hours, which means that the heat treatment has the maximum efficiency at 20 hours temperature maintenance.
- Physico-chemical analyzes of HEA3 and HEA4 alloy samples processed in vacuum induction furnace indicate a change in the properties of the alloys depending on the Al and Zr content of them. Thus, at a content of Al 6.66 at.% and 4.44 at.% Zr, respectively, the HEA3 alloy has a hardness in the cast state of 558.1 HV and is composed mostly of phase A2 with crystalline structure CVC with lower additives of C15 Laves and A12 phases. After the heat treatment at 700 ℃ for 20 hours, the measured hardness shows an increase of 447.5HV, respectively 80.18%. In the case of the HEA4 alloy which has a low contents of Al 4.65at.% and 2.32at.% Zr, respectively, its measured hardness in the cast state is 358.2HV for HEA4Cu and 388.4HV for HEA4Gr. The alloys mostly have a A1 type solid solution phase with CFC structure

and lower contents of phase A2 and C15 Laves. After the same heat treatment, their hardness increases by 450.8HV - 414HV and 125.85% - 106.59%, respectively

- In the case of heat treatments at higher temperatures (1100 ° C) the HEA3 alloy shows a decrease in hardness reaching values even below those specific to the as-cast alloy.
- In the case of HEA3 alloy, by correlating the DRX and EDS data, the formation of the majority dendritic structure from phase A2 (Cr, Fe, Ni) can be discussed. At the same time, the association of the solid solution phases A2 and C15 determined by XRD with the eutectic identified by optical and electron microscopy can be interpreted.
- Hard compounds appear in the HEA3 alloy sample that can be justified by the high concentration of zirconium, as can be seen in the EDS analysis.
- By changing the chemical composition, the deformability properties of HEA alloys can be controlled and improved. Thus, after decreasing the Al and Zr content, the DRX analysis indicates the appearance of a A1 type solid solution phase with ductile FCC structure.
- Following the hot rolling and forging process, the HEA4 alloy does not show major changes in the microstructure. Due to the higher amount of solid solution type A1 FCC, the HEA4Cu alloy had higher deformability than HEA4Gr. Thus the height of the HEA4Cu sample was reduced by 49.3% compared to the 24% reduction in the height of the HEA4Gr alloy
- The DRX analysis on the heat-treated samples confirms the results of the calculation of the PSFE criterion for the occurrence of sigma-type phases in HEA3 and HEA4 alloys.
- Oxidation resistance testing processes suggest that a higher aluminum and zirconium content increases the oxidation resistance of HEA alloy. Thus, HEA3 and HEA3R alloys obtained the best results after oxidation.
- Increasing the content of Al and Zr positively influences the oxidation properties of alloys but has a negative influence in the case of plastic deformation properties.

Personal contributions

- Approach of three new HEA alloy systems: Cr - Fe - Ni - Nb - W - HEA1, Cr - Fe - Ni - Mo - W - HEA2, and Al - Cr - Fe - Mn - Ni - Zr - HEA3 and HEA4 for the study of physico-chemical and mechanical properties. HEA-specific thermodynamic criteria were calculated: entropy of mixing, enthalpy of mixing, in atomic radius difference, the difference in electronegativity, valence electrons concentration,
- Influence of Al and Zr alloying elements in the Al - Cr - Fe - Mn - Ni - Zr system was studied in order to obtain alloys with physical properties compatible with sheet metal processing processes. The influence of Nb and Mo elements in the Cr-Fe-Ni-Mex-W system on the tensile strength was also studied.
- Thermodynamic and kinetic modelling was performed using MatCalc and Thermocalc software for the alloys:
  o Cr2.94Fe2.74Ni3.65Nb0.32W0.33 - HEA1,
  o Cr2.94Fe2.74Ni3.65Mo0.31W0.33 - HEA2,
  o Al0.3CrFeMnNiZr0.2 - HEA3 and
  o Al0.2CrFeMnNiZr0.1 - HEA4,
  in order to obtain the the alloys constituent phases, the precipitated phases following the heat treatments, but also to study the influence of the alloying elements.

- The experimental model for obtaining high entropy alloys in induction furnace and their heat treatment to improve mechanical properties was developed.
- The influence of the heat treatment temperature on the microstructure and mechanical properties of the alloys Al0.3CrFeMnNiZr0.2 - HEA3 and Al0.2CrFeMnNiZr0.1 - HEA4 was studied.
- Vacuum heat treatments were performed to improve the mechanical properties of HEA1 and HEA2 alloys, which resulted in an increase in mechanical tensile strength.
- Oxidation studies were performed on all 4 HEA samples intended for the manufacture of combustion chambers of thermal power plants.

Further research perspectives

Studies for the development of new high entropy alloys for high-temperature applications will be continued in two main directions:

1. Development of HEA alloys for high temperature resistant thin film coatings of jet engine parts and combustion chamber parts in thermal power plants.

2. Development of HEA alloys specially designed for SEBM additive manufacturing technique with powder bed. Also, research will continue on the mechanical properties of the alloys studied in this paper through tests on tensile, creep, cavitation and wear and on the influence of alloying elements correlated with the resulting mechanical properties.

At the same time, corrosion and oxidation studies will be performed at high temperatures. The studies will use thermodynamic and kinetic modelling programs, and the results will be put into practice by melting and casting in vacuum induction furnace, levitation furnace and electric arc furnace.

Results disemination

Scientific papers presented at national and international conferences

- D. Mitrica, V. Soare, I. Constantin, **M. Olaru**, V. Badilita, V. Soare, F. Stoiciu, G. Popescu, I. Carcea, *Influence of the heat treatment processes on the properties of high entropy alloys based on Al-Cr-Fe-Mn-Ni system*, The 3rd Mediterranean Conference on Heat Treatment and Surface Engineering – MCHTSE2016, 26-28 September 2016, Portoroz, Slovenia
- D. Mitrica, V. Soare, D. Dumitrescu, V. Soare, G. Popescu, I. Constantin, **M. Olaru**, M. Ghita, B. Ghiban E. Vasile, *New high entropy alloys with superior characteristics*

for medical applications, European Congress and Exhibition on Advanced Materials and Processes – EUROMAT 2017, 17–22 September 2017, Thessaloniki, Greece

- D. Mitrica, V. Soare, **M. T. Olaru**, V. Dragut, G. Popescu, C. Predescu, A. Berbecaru, Vi. Soare, M. Ghita, *Influence of the element additions to the microstructural and mechanical characteristics of selected high entropy alloys*, 10th International Conference on Materials Science & Engineering – BraMat 2017, 8 – 11 March 2017, Brasov, Romania
- **M. Olaru**, V. Soare, D. Mitrica, V. Dragut, F. Stoiciu, G. Popescu, I. Carcea, *Heat treatment and deformability of Al-Cr-Fe-Mn-Ni-Zr high entropy alloys*, European Congress and Exhibition on Advanced Materials and Processes – EUROMAT 2017, 17–22 September 2017, Thessaloniki, Greece
- D. Mitrica, V. Soare, **M. T. Olaru**, G. Popescu, C. Predescu, I. Carcea, V. Badilita, V. I. Soare, F. Stoiciu, *High entropy alloys for steam power plant applications*, The 5th International Conference on Modern Manufacturing Technologies in Industrial Engineering-ModTech 2017, 14-17 June 2017, Sibiu, Romania
- D. Mitrică, V. Soare, I. Constantin, **M. Olaru**, B. A. Cârlan, M. Ghiță, V. D. Dragut, *Structural Particularities of Low Density High Entropy Alloys*, 4th Global Congress & Expo on Materials Science and Nanoscience – MSN 2018, 15-17 October 2018, Amsterdam, Netherlands
- **M. T. Olaru**, D. Mitrică, B. A. Cârlan, M. Ghiță, V. D. Dragut, *E-beam co-deposition of Al0.3CrFeMnNiZr0.2 High Entropy Alloy Thin Film*, 4th Global Congress & Expo on Materials Science and Nanoscience – MSN 2018, 15-17 October 2018, Amsterdam, Netherlands
- D. Mitrică, V. Soare, I. Constantin, **M. Olaru**, B. A. Cârlan, M. Ghiță, V. D. Dragut, Structural Particularities of Low Density High Entropy Alloys, 4th Global Congress & Expo on Materials Science and Nanoscience – MSN 2018, 15-17 October 2018, Amsterdam, Netherlands
- **Mihai T. Olaru**, D. Mitrica, V. Soare , I. Constantin, M. Burada , D. Dumitrescu, A. Caragea, B. A. Carlan, C. I. Banica, F. Stoiciu, V. Badilita, V. Geanta, R. Stefanoiu, *Synthesis and characterization of high entropy alloys for high temperature applications*, 7th International Conference on Materials Science and Technologies – RoMat 2018, November 15-18-th, 2018, Bucharest, Romania
- **M. T. Olaru**, D. Mitrica, I. Constantin, C. Banica, M. Burada, D. V. Dumitrescu, B. A. Carlan, *Influence of heat treatment on Al0.5Cr0.5Ni0.5TZr1.5Nb1.5 high entropy alloy*, 7th International Conference on Modern Manufacturing Technologies in Industrial Engineering - ModTech 2019, 19 -22 June 2019, Iasi, Romania
- **Olaru M.T**., Mitrica D., Piticescu R., Carlan B., Banica C., Denisa V., Sluiter M., Podgronik B., Badilita V., Dragut V., Stoiciu F., Ghita M., *Microstructure and properties of Al2CrNbTiZrW0.3 and Al2CoNbTiZrW0.3 high entropy alloys*, EUROMAT2019, Stockholm, Suedia, 1-5 sept. 2019
- Cristina – Ioana Banica, Dumitru Mitrica, **Mihai – Tudor Olaru**,Beatrice – Adriana Carlan,Denisa Vonica,Lidia Licu,Marian Burada,Daniela Dumitrescu,Victor Geanta,Adrian Rotariu,Elena Scutelnicu,Danut Savu,Florentin Stoiciu,Valentin – Dumitru Dragut,Laura, Eugenia Barbulescu, *Structure and properties of a new low weight high entropy alloy,* EUROMAT2019, Stockholm, Suedia, 1-5 sept. 2019

Articles published in specialized journals

Articles published in ISI journals

- Mitrica, D.; Badea, I.C.; **Olaru, M.T**.; Serban, B.A.; Vonica, D.; Burada, M.; Geanta, V.; Rotariu, A.N.; Stoiciu, F.; Badilita, V.; Licu, L. *Modeling and Experimental Results of Selected Lightweight Complex Concentrated Alloys, before and after Heat Treatment. Materials* 2020, *13*, 4330, https://doi.org/10.3390/ma13194330

- **Mihai Tudor Olaru**, **Mihail Tarcolea**, Dumitru Mitrica, Marian Burada, Daniela Dumitrescu, Cristina Banica, Beatrice Carlan, *Influence of heat treatment on* $Al_{0.5}Cr_{0.5}Ni_{0.5}TiZr_{1.5}Nb_{1.5}$ *high entropy alloy*, U.P.B. Scientific Bulletin Series B, vol. 82, no. 2 (2020). Emerging Sources Citation Index (Web of Science).

- **M. T. Olaru**, D. Mitrica, V. Soare, I. Constantin, M. Burada, D. Dumitrescu, A. Caragea, B. A. Carlan, C. I. Banica, F. Stoiciu, V. Badilita, V. Geanta, R. Stefanoiu, *"Synthesis and characterization of high entropy alloys for high temperature applications",* U.P.B. Scientific Bulletin Series B, vol. 81, no. 2 (2019), 249-256. Emerging Sources Citation Index (Web of Science)

- Mitrica D., **Olaru M. T**., Dragut V., Predescu C., Berbecaru A., Ghita M., Carcea I., Burada M., Dumitrescu D., Șerban (Cârlan) B. A., Banica C. I., *Influence of composition and as – cast structure on the mechanical properties of selected high entropy alloys*, Materials Chemistry and Physics, 242, 2020, 122555, https://doi.org/10.1016/j.matchemphys.2019.122555

- D. Mitrica, V. Soare, I. Constantin, M. Burada, **M. Olaru**, V. Badilita, V. Soare, F. Stoiciu, G. Popescu, and I. Carcea, *Influence of the Heat Treatment Processes on the Properties of High Entropy Alloys Based on Al-Cr-Fe-Mn-Ni System*, Materials Performance and Characterization 6, no. 5 (2017): 823-836. Emerging Sources Citation Index (Web of Science), https://doi.org/10.1520/MPC20170018

- G. Popescu , B. Ghiban, C. A. Popescu, L. Roșu, R. Trușcă, I. Carcea, V. Soare, D. Dumitrescu, I. Constantin, **M. T. Olaru,** B. A. Cârlan, *New TiZrNbTaFe high entropy alloy used for medical applications*, IOP Conference Series: Materials Science and Engineering, vol. 400 (2018), 022049, doi:10.1088/1757-899X/400/2/022049

- B Ghiban, G Popescu, C Lazar, L Rosu, I Constantin, **M Olaru**, B Carlan, *Corrosion behaviour in human stimulation media of a high entropy titan-based alloy*, IOP Conference Series: Materials Science and Engineering, vol. 374 (2018), 012004, doi:10.1088/1757-899X/374/1/012004

Articles published in non-ISI journals

- V. Soare, D. Mitrica, I. Constantin, **M. T. Olaru**, V. Soare, B. A. Carlan, M. Ghita, G. Popescu, I. Carcea, *Influenta condițiilor de turnare asupra microstructurii si proprietăților aliajelor cu entropie înaltă din sistemul Al-Cr-Fe-Mn-Ni-Zr*, Revista de Turnătorie, nr 4, 2018, pag 18-33,CZU 621.74 (051) ISSN 1224 – 21 – 44.

Patent applications

- Aliaj cu entropie inalta pentru aplicatii la temperaturi inalte și procedeu de obținere", Mitrica Dumitru, **Olaru Mihai**, Piticescu Radu Robert, Burada Marian, Dumitrescu Daniela Violeta, Șerban (Cârlan) Beatrice Adriana, Enache Gabriel, cerere OSIM, cu numărul A00590/24.09.2019.
- "Procedeu de obtinere aliaj cu entropie inaltă, prelucrabil si cu duritate ridicata, pentru fabricarea de role de laminor", D. Mitrica, V. Soare, A. Caragea, **M. Olaru**, I. Carcea, R. Chelariu, M. Gherghe, M. Sarghi, G. Popescu, I. Csaki, RO20160000942
- „Aliaje Sb-Te-Zn-Sn cu proprietăți termoelectrice și procedeu de obținere", M. Burada, I. Constantin, D. Mitrică, **M. Olaru**, D. Dumitrescu, V. Soare, M. Ghiță, V. Drăguț, RO20170000906 20171108
- „Filme subțiri din aliaje Sn-Ni pentru anozi utilizați in baterii litiu-ion și procedeu de obținere", M.L. Soare, M. Burada, I. Constantin, **M. Olaru**, A. Sobetkii, P. Capota, A. N. Lupu, D. V. Drăguț, RO20170001059 20171208

Bibliography

[1] Murty, B.S. & Yeh, Jien-Wei & Ranganathan, Srinivasa. (2014). A Brief History of Alloys and the Birth of High-Entropy Alloys. 10.1016/B978-0-12-800251-3.00001-8.

[2] Jien-Wei Yeh, Swe-Kai Chen, Su-Jien Lin, Jon-Yiew Gan, Tsung-Shune Chin, Tao-Tsung Shun, Chun-Huei Tsau, and Shou-Yi Chang "Nanostructured High-Entropy Alloys with Multiple Principal Elements: Novel Alloy Design Concepts and Outcomes", Advanced Engineering Materials, vol. 6, issue 5, 2004.

[3] Gaskell DR "Introduction to the thermodynamics of materials", 3rd edn. Taylor & Francis Ltd, Washington, DC, pp 80–84, 1995.

[4] Swalin RA "Thermodynamics of solids", 2nd edn. Wiley, New York, pp 35–41, 1972.

[5] B.S. Murty, J.W. Yeh, S. Ranganathan, „High entropy alloys", 2014, ISBN:9780128002513

[6] Cullity, B.D., Stock, S.R., "Elements of X-Ray Diffraction", Prentice Hall, New Jersey, USA, 2001.

[7] Reed-Hill, R.E., Abbaschian, R., "Physical Metallurgy Principles", PWS Publishing, Boston, USA, 1994.

[8] Yeh JW. Recent progress in high-entropy alloys. Presentation at Changsha meeting; 2011.

[9] Massalski, T.B., "Phase diagrams in materials science", Metall. Trans. A 20A, 1295_1323, 1989.

[10] Yeh, J.W., Chen, S.K., Lin, S.J., Gan, J.Y., Chin, T.S., Shun, T.T., et al., "Nanostructured high-entropy alloys with multiple principal elements: novel alloy design concepts and outcomes", Adv. Eng. Mater. 6, 299_303, 2004.

[11] International Iron and Steel Institute. Committee on Technology, "The Electric Arc Furnace", The Institute, 1981

[12] Annie Gagnoud, Jacqueline Etay, Marcel Garnier, "The levitation melting process using cold crucible technique", The Iron and Steel Institute of Japan, 1987

[13] C. Suryanarayana, "Mechanical alloying and milling", Progress in Materials Science, vol. 46, 1-184, 2001

[14] F.H. Froes, *Structural Applications of Mechanical Alloying*, Ed: F.H. Froes and J.J. deBarbadillo, Proceedings of an ASM Intern. Confer., Myrtle Beach, South Carolina, 27-29 March 1990

[15] A. Essienubong, O. Ikechukwu, P. O. Ebunilo, E. Ikpe, „Material Selection for High Pressure (HP) Turbine Blade of Conventional Turbojet Engines", American Journal of Mechanical and Industrial Engineering, vol. 1, no. 1 (2016), 1-9.

[16] J. C. Zhao, J. H. Westbrook, „Ultrahigh-Temperature Materials for Jet Engines", MRS BULLETIN, 2003, 622-626.

[17] R. Schafrik, R. Sprague, "Saga of Gas Turbine Materials: Part III", Advanced Materials and Processes, vol. 162 (2004), 27–30.

[18] F. Campbell, „Manufacturing Technology for Aerospace Structural Material", Elsevier London, 2006.

[19] R. Flack, „Fundamental of Jet Propulsion with Applications. Chapter 8: Axial Flow Turbines", Cambridge University Press, New York, 2005.

[20] R. Agarwal, „Recent Advances in Aircraft Technology", InTech, Rijeka, Croatia, 2012.

[21] K. A. Christofidou, N. G. Jones, E. J. Pickering, R. Flacau, M. C. Hardy, H. J. Stone, „The microstructure and hardness of Ni-Co-Al-Ti-Cr quinary alloys", Journal of Alloys and Compounds, vol. 688 (2016), 542-552.

[22] Maziasz, P. & Wright, Ian & Shingeldecker, J. & Gibbons, T. & Romanosky, R.." Defining the Materials Issues and Research for Ultra-Supercritical Steam Turbines".

Proceedings of the 4th International Conference on Advances in Materials Technology for Fossil Power Plants. 2005.

[23] R. Viswanathan, J.F. Henry, J. Tanzosh, G. Stanko, J.P. Shingledecker, and B. Vitalis, "Materials for Ultrasupercritical Coal Fired Power Plant Boilers," Proceedings of the 29th Internat. Conf. on Coal Utilization and Fuel Systems, held April 18-23, 2004 in Clearwater, FL, Coal Technology Association, Gaithersburg, MD 20878.

[24] R. Blum and R.W. Vanstone, "Materials Development for Boilers and Steam Turbines Operating at 700oC," in Parsons 2003 – Engineering Issues in Turbine Machinery, Power Plant and Renewables, Institute for Materials, Minerals and Mining, Maney Publishing, London, England, 2003, p. 489-510.

[25] I.G. Wright, P.J. Maziasz, F.V. Ellis, T.B. Gibbons, and D.A. Woodford, "Materials Issues for Turbines for Operations in Ultra-Supercritical Steam," Proceedings of the 29th Internat. Conf. on Coal Utilization and Fuel Systems, held April 18-23, 2004 in Clearwater, FL, Coal Technology Association, Gaithersburg, MD 20878.

[26] P.J. Maziasz, I.G. Wright, J.P. Shingledecker, T.B. Gibbons, and R.R. Romanosky, "Defining the Materials Issues and Research Needs for Ultra-Supercritical Steam Turbines," Proc. 4th Internat. Conf. Advances in Materials Technology for Fossil Power Plants, EPRI Conference, ASM-International, Materials Park, OH (2005) pp. 602-622.

[27] Yeh J.W., Chen Y.L., Lin S.J., Chen S.K., "*High-Entropy Alloys – A New Era of Exploitation"*, Mater. Sci. Forum. 560, 1–9, 2007.

[28] Wu J.M., Lin S.J., Yeh J.W., Chen S.K., Huang Y.S., Chen H.C., "*Adhesive wear behavior of AlxCoCrCuFeNi high-entropy alloys as a function of aluminium content"*, Wear. 261, 513–519, 2006.

[29] Zhou Y.J., Zhang Y., Wang Y.L., Chen G.L., "*Microstructure and compressive properties of multicomponent Alx(TiVCrMnFeCoNiCu)100−x high-entropy alloys"*, Mater. Sci. Eng. A. 454–455, 260–265, 2007.

[30] Tong C.J., Chen Y.L., Yeh J.W., Lin S.J., Chen S.K., Shun T.T., Tsau C.H., Chang S.Y., "*Microstructure characterization of AlxCoCrCuFeNi high-entropy alloy system with multiprincipal elements"*, Metall. Mater. Trans. A. 36, 881–893, 2005.

[31] Wang W.R., Wang W.L., Wang S.C., Tsai Y.C., Lai C.H., Yeh J.W., "*Effects of Al addition on the microstructure and mechanical property of AlxCoCrFeNi highentropy alloys"*, Intermetallics. 26, 44–51, 2012.

[32] Tong C.J., Chen M.R., Yeh J.W., Lin S.J., Chen S.K., Shun T.T., Chang S.Y., "*Mechanical performance of the AlxCoCrCuFeNi high-entropy alloy system with multiprincipal elements"*, Metall. Mater. Trans. A. 36, 1263–1271, 2005.

[33] Zhang K.B., Fu Z.Y., Zhang J.Y., Wang W.M., Wang H., Wang Y.C., Zhang Q.J., Shi J., "*Microstructure and mechanical properties of CoCrFeNiTiAlx highentropy alloys"*, Mater. Sci. Eng. A. 508, 214–219, 2009.

[34] Wu J.M., Lin S.J., Yeh J.W., Chen S.K., Huang Y.S., Chen H.C., "*Adhesive wear behavior of AlxCoCrCuFeNi high-entropy alloys as a function of aluminium content"*, Wear. 261, 513–519, 2006.

[35] Tung C.C., Yeh J.W., Shun T., Chen S.K., Huang Y.S., Chen H.C., "*On the elemental effect of AlCoCrCuFeNi high-entropy alloy system"*, Mater. Lett. 61, 1–5, 2007.

[36] Zhou Y.J., Zhang Y., Wang Y.L., Chen G.L., "*Solid solution alloys of AlCoCrFeNiTix with excellent room-temperature mechanical properties"*, Appl. Phys. Lett. 90, 2007.

[37] Wang X.F., Zhang Y., Qiao Y., Chen G.L., "*Novel microstructure and properties of multicomponent CoCrCuFeNiTix alloys"*, Intermetallics. 15, 357–362, 2007.

[38] Chen M.R., Lin S.J., Yeh J.W., Chen S.K., Huang Y.S., Tu C.P., *Microstructure and properties of Al0.5CoCrCuFeNiTix (x = 0-2.0) high-entropy alloys*, Mater. Trans. 47, 1395–1401, 2006.

[39] Hsu C.Y., Sheu T.S., Yeh J.W., Chen S.K., "*Effect of iron content on wear behavior of AlCoCrFexMo0.5Ni high-entropy alloys"*, Wear. 268, 653–659, 2010.

[40] Ma S.G., Zhang Y., "*Effect of Nb addition on the microstructure and properties of AlCoCrFeNi high-entropy alloy"*, Mater. Sci. Eng. A. 532, 480–486, 2012.

[41] Wang F.J., Zhang Y., "*Effect of Co addition on crystal structure and mechanical properties of Ti0.5CrFeNiAlCo high entropy alloy"*, Mater. Sci. Eng. a-Structural Mater. Prop. Microstruct. Process. 496, 214–216, 2008.

[42] Li B.S., Wang Y.P., Ren M.X., Yang C., Fu H.Z., *Effects of Mn, Ti and V on the microstructure and properties of AlCrFeCoNiCu high entropy alloy*, Mater. Sci. Eng. A. 498, 482–486, 2008.

[43] Chen M.R., Lin S.J., Yeh J.W., Chuang M.H., Chen S.-K., Huang Y.-S., "*Effect of vanadium addition on the microstructure, hardness, and wear resistance of Al0.5CoCrCuFeNi high-entropy alloy"*, Metall. Mater. Trans. A. 37, 1363– 1369, 2006.

[44] GUO S., HU Q., Ng C. and LIU C. T., More than entropy in high-entropy alloys: Forming solid solutions or amorphous phase. Intermetallics 41, 96–103 (2013).

[45] YANG X. and ZHANG Y., "Prediction of high-entropy stabilized solid-solution in multi-component alloys", Materials Chemistry and Physics, Vol. 132, No 2-3, 2012, pp233–238.

[46] M.-H. Tsai, K.-C. Chang, J.-H. Li, R.-C. Tsai, and A.-H. Cheng, "A second criterion for sigma phase formation in high-entropy alloys," *Mater. Res. Lett.*, vol. 3831, no. April, pp. 1–6, 2015.

[47] M. H. Tsai, J. H. Li, A. C. Fan, and P. H. Tsai, "Incorrect predictions of simple solid solution high entropy alloys: Cause and possible solution," *Scr. Mater.*, vol. 127, pp. 6–9, 2017.

[48] Senkov, O. N. & Miracle, D. B., "A new thermodynamic parameter to predict formation of solid solution or intermetallic phases in high entropy alloys", *Journal of Alloys and Compounds,*Vol. 658, 2016, pp. 603–607.

[49] Miracle DB, Miller JD, Senkov ON, Woodward C, Uchic MD, Tiley J "Exploration and development of high entropy alloys for structural applications", Entropy 16:494–525, 2014.

[50] Zhang, K.B., Fu, Z.Y., Zhang, J.Y., Shi, J., Wang, W.M., Wang, H., et al., "Annealing on the structure and properties evolution of the CoCrFeNiCuAl high-entropy alloy", J. Alloys Compd. 502, 295_299, 2010.

[51] Zhang K., Fu Z., "*Effects of annealing treatment on phase composition and microstructure of CoCrFeNiTiAlx high-entropy alloys"*, Intermetallics. 22, 24–32, 2012.

[52] Pi J.H., Pan Y., Zhang L., Zhang H., "*Microstructure and property of AlTiCrFeNiCu high-entropy alloy"*, J. Alloys Compd. 509, 5641–5645, 2011.